MEASUREMENTS OF THE RATIOS OF INTERNAL CONVERSION COEFFICIENTS OF CASCADE TRANSITIONS FOLLOWING ELECTRON CAPTURE BY A SUM COINCIDENCE TECHNIQUE

A Thesis

Submitted to the

Faculty of Graduate Studies

In Partial Fulfillment

of the Requirements for the Degree of

Master of Science

at

The University of Manitoba

---

by

D. Roger Brundrit

Winnipeg, Canada

December 1964

PREFACE AND ACKNOWLEDGEMENTS

This thesis has been written in two parts. Part I contains the theory, description and results of an experiment to measure the ratios of the conversion coefficients of cascade gamma rays using a new sum coincidence technique. To do this work a solid state electron detector was used, the properties of which were not fully known. Part II contains the work carried out on the electron detector, this work being directed primarily in such a way as to yield that data concerning the detector which was necessary to complete Part I of this thesis.

I must first express my sincere gratitude to Dr. S. K. Sen for his helpful and extremely enthusiastic supervision throughout this work. I wish also to thank Dr. K. I. Roulston for many constructive discussions, Dr. R. D. Connor for the use of the beta ray spectrometer and Dr. B. G. Hogg for the use of the multi-channel analyser. I am deeply indebted to Mr. R. D. Ross for his help with the work on the beta ray spectrometer and to Dr. D. P. Kerr for his friendly and valuable assistance on many occasions. My thanks are also due to the National Research Council of Canada for some financial assistance in carrying out this work.

TABLE OF CONTENTS

LIST OF FIGURES

LIST OF TABLES

ABSTRACT

A recently proposed sum coincidence technique, for the direct measurement of the ratios of internal conversion coefficients of cascade transitions, has been shown to yield values for these ratios which are in excellent agreement with those obtained by other methods. This new method is independent of the relative intensities of the cascade transitions and of the half life of the parent isotope. Cascade transitions in the levels of As^{75} and Cs^{131} have been studied.

The ratios of the total internal conversion coefficients for cascades from the 401 keV level in As^{75} have been found to be: $\frac{\alpha_{121}}{\alpha_{280}} = 5.5 \pm 0.6$; and $\frac{\alpha_{136}}{\alpha_{265}} = 4.0 \pm 0.3$.

The value obtained for the ratios of the K conversion coefficients of the 124 keV - 496 keV cascade in Cs^{131} was 65 ± 5.

Measurements on the K/(L+M) ratios for the 124, 216, 373 and 496 keV transitions in Cs^{131} yielded the following values:

$$\left(K/(L+M) \right)_{124} = 2.6 \pm 0.2; \quad \left(K/(L+M) \right)_{216} = 3.1 \pm 0.3;$$

$$\left(K/(L+M) \right)_{373} = 4.6 \pm 0.5; \quad \left(K/(L+M) \right)_{496} = 6.1 \pm 0.5.$$

INTRODUCTION

A knowledge of the internal conversion coefficients, or their ratios, is of importance to obtain some picture of the excited states of a particular nucleus. Theoretically, from the internal conversion coefficients of transitions it is possible to predict the spin and parity changes involved in nuclear transitions, and hence the experimental values of the internal conversion coefficients provide a good test for the theories of nuclear energy levels. In this thesis is presented a direct method of measuring the ratio of the internal conversion coefficients of cascade transitions. The method has been applied here only to cascade transitions following electron capture as the beta spectra are much simplified for this type of decay.

The method described in this thesis utilizes a sum coincidence technique and has the following main advantages over the usual method employing a beta ray spectrometer.

i) It is a direct method since it involves only one experimental measurement as opposed to other methods which require a knowledge of both the conversion electron and the gamma ray intensities.

ii) The method is independent of the half life of the decaying parent isotope.

THEORY OF THE SUM COINCIDENCE TECHNIQUE

This method of measuring internal conversion coefficients of cascade transitions by a sum coincidence technique was proposed by S. K. Sen[1] and subsequently reported by Sen and Hogg[2]. The method relies upon a sum coincidence between a conversion electron from one part of the cascade and a gamma ray from the other part as shown in Fig. 1.

Fig. 1:
Simple Cascade Transition

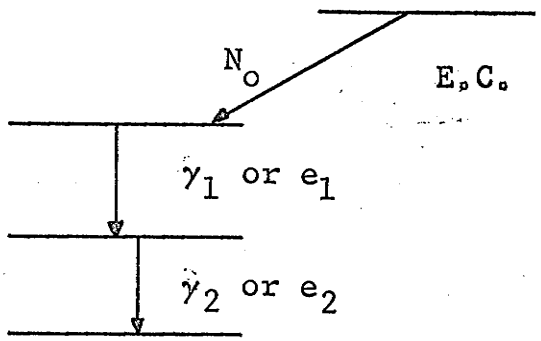

Electron capture sources had the advantage that all electron gamma coincidences that were observed were from cascade transitions. The internal conversion coefficient, α, is defined by the equation:-

$$\alpha = \frac{N_e}{N_\gamma}$$

where:

N_e is the number of conversion electrons and N_γ is the number of gamma rays from the same transition. If we consider a simple cascade transition, such as that shown in

Fig. 1, then the following equations can be deduced:

$$N_{e_1} = \frac{N_o}{(1 + \alpha_1)} \cdot \alpha_1 \cdot {}^{e}\beta_1 \cdot \omega_\beta \qquad \ldots (1)$$

where:

N_{e_1} is the number of conversion electrons from the first transition which give a pulse in the total absorption peak of the electron detector;

N_o is the number of cascade transitions;

α_1 is the conversion coefficient of the first transition;

${}^{e}\beta_1$ is the peak efficiency of the electron detector for conversion electrons from the first transition;

and ω_β is the solid angle of the electron detector, as seen by the source.

Similarly, for conversion electrons from the second transition:

$$N_{e_2} = \frac{N_o}{(1 + \alpha_2)} \cdot \alpha_2 \cdot {}^{e}\beta_2 \cdot \omega_\beta \qquad \ldots (2)$$

If we now look for coincidences between conversion electrons of the first transition and the following cascade gamma ray we obtain:

$$N_{e_1 \gamma_2} = N_{e_1} \cdot \frac{1}{(1 + \alpha_2)} \cdot {}^{e}\gamma_2 \cdot \omega_\gamma \qquad \ldots (3)$$

where:

$N_{e_1 \gamma_2}$ is the number of pulses of type N_{e_1} which are recorded in coincidence with a photo-peak pulse in the gamma detector caused by a gamma ray from the second part of the cascade;

e_{γ_2} is the photo-peak efficiency of the gamma detector for photons from the second transition;

and ω_γ is the solid angle of the gamma detector as seen by the source.

Similarly, for coincidences between a conversion electron from the second transition and the preceeding gamma ray, we obtain:

$$N_{e_2 \gamma_1} = N_{e_2} \cdot \frac{1}{(1 + \alpha_1)} \cdot e_{\gamma_1} \cdot \omega_\gamma \qquad \ldots (4)$$

Dividing equation (3) by equation (4) and substituting for N_{e_1} and N_{e_2} from equations (1) and (2), we obtain:

$$\frac{N_{e_1 \gamma_2}}{N_{e_2 \gamma_1}} = \frac{\alpha_1}{\alpha_2} \cdot \frac{e_{\beta_1}}{e_{\beta_2}} \cdot \frac{e_{\gamma_2}}{e_{\gamma_1}} \qquad \ldots (5)$$

If we now display these coincidence pulses from the electron detector on a multi-channel pulse height analyzer, we will get an area A_1 corresponding to $N_{e_1 \gamma_2}$ and an area A_2 corresponding to $N_{e_2 \gamma_1}$ so that equation (5) can be written as:

$$\frac{\alpha_1}{\alpha_2} = \frac{A_1}{A_2} \cdot \frac{e_{\beta_2}}{e_{\beta_1}} \cdot \frac{e_{\gamma_1}}{e_{\gamma_2}} \qquad \ldots (6)$$

Hence we are able to find $\frac{\alpha_1}{\alpha_2}$.

By dividing equation (1) by equation (2) we obtain:

$$\frac{N_{e_1}}{N_{e_2}} = \frac{\alpha_1}{\alpha_2} \cdot \frac{N_o}{(1+\alpha_1)} \cdot \frac{1+\alpha_2}{N_o} \cdot \frac{e_{\beta_1}}{e_{\beta_2}} \qquad \ldots (7)$$

From the singles electron spectrum displayed on a multi-channel analyser we can obtain the areas A_1' and A_2' corresponding to N_{e_1} and N_{e_2} respectively in equation (7), so that:

$$\frac{N_o}{1+\alpha_1} \cdot \frac{1+\alpha_2}{N_o} = \frac{A_1'}{A_2'} \cdot \frac{\alpha_2}{\alpha_1} \cdot \frac{e_{\beta_2}}{e_{\beta_1}} \qquad \ldots (8)$$

Now $\frac{N_o}{1+\alpha_1} = N_{\gamma_1}$ for this simple cascade,

$$\therefore \frac{N_{\gamma_1}}{N_{\gamma_2}} = \frac{A_1'}{A_2'} \cdot \frac{e_{\beta_2}}{e_{\beta_1}} \cdot \frac{\alpha_2}{\alpha_1} \qquad \ldots (9)$$

thus enabling us to find the ratio of the gamma ray intensities of the two transitions.

There are however very few decay schemes of the simple type shown in Fig. 1 and it is shown below how equations (6) and (9) may be derived in the case of a more complicated decay scheme shown in Fig. 2.

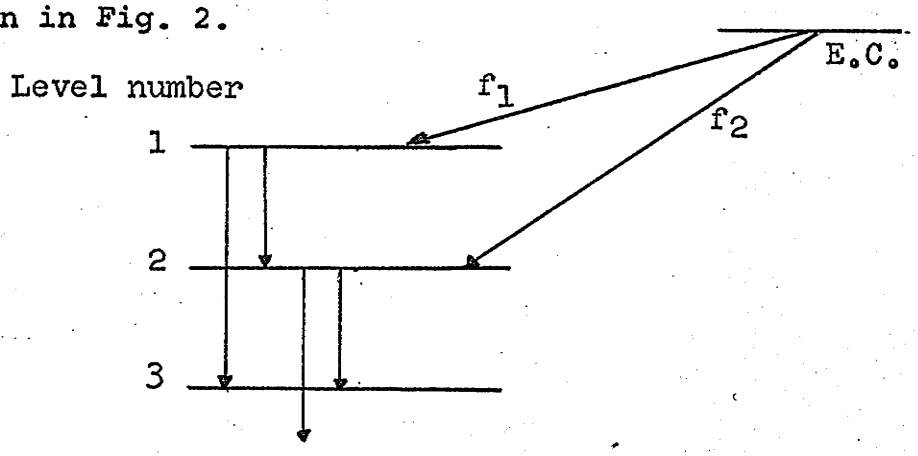

Fig. 2:
Complex cascade transition.

Suppose we are interested in the cascade from level 1 to level 3 via level 2.

Let the fraction of transitions from level 1 to level 2 be X_1, and from level 2 to level 3 be X_2.

If we consider first the equations for a sum coincidence then the number of conversion electrons from the 1 to 2 transition is equal to $\frac{N_{o1}\alpha_1}{(1+\alpha_1)}$ where N_{o_1} is the total number of transitions from level 1 to level 2 and is equal to $X_1 f_1 N_o$ where N_o is the total number of decays, and f_1 is the fraction of the total number of electron capture transitions leading to level 1.

Hence equation (1) will become:-

$$N_{e_1} = N_{o1} \frac{\alpha_1}{(1+\alpha_1)} \cdot e_{\beta_1} \cdot \omega_\beta \qquad \ldots (10)$$

The proportion of transitions from level 1 to level 2 followed by a transition from 2 to 3 is X_2 and equation (3) becomes:-

$$N_{e_1\gamma_2} = N_{e_1} \cdot x_2 \cdot \frac{1}{(1+\alpha_2)} \cdot e_{\gamma_2} \cdot \omega_\gamma \qquad \ldots (11)$$

The number of gamma rays from level 1 to level 2 is $\frac{N_{o1}}{1+\alpha_1}$ and the proportion of these followed by a 2 to 3 transition is X_2 and equation (4) becomes:-

$$N_{e_2\gamma_1} = \frac{N_{o1}}{(1+\alpha_1)} \cdot e_{\gamma_1} \omega_\gamma \cdot \frac{x_2 \alpha_2}{(1+\alpha_2)} \cdot e_{\beta_2}\omega_\beta \qquad \ldots (12)$$

Dividing (11) by (12) and substituting for N_{e_1} using equation (10) we obtain:-

$$\frac{N_{e_1\gamma_2}}{N_{e_2\gamma_1}} = \frac{\alpha_1}{\alpha_2} \cdot \frac{e_{\beta_1}}{e_{\beta_2}} \cdot \frac{e_{\gamma_2}}{e_{\gamma_1}} \qquad \ldots (13)$$

which is identical to equation (5).

In the case of the singles, we have already found N_{e_1} for this complex decay scheme and this is given in equation (10). In this equation we can substitute N_{γ_1} for $\frac{N_{o1}}{(1+\alpha_1)}$ to obtain:-

$$N_{e_1} = N_{\gamma_1} \cdot \alpha_1 \cdot e_{\beta_1} \cdot \omega_\beta \qquad \ldots (14)$$

and similarly we write for the total number of transitions from level 2 to level 3, $N_{o_2} = X_2 N_o (X_1 f_1 + f_2)$ and then $N_{\gamma_2} = \frac{N_{o2}}{(1+\alpha_2)}$ so that, $N_{e_2} = N_{\gamma_2} \cdot \alpha_2 \cdot e_{\beta_2} \cdot \omega_\beta \qquad \ldots (15)$

Dividing equation (14) by (15) we obtain:-

$$\frac{N_{e_1}}{N_{e_2}} = \frac{N_{\gamma_1}}{N_{\gamma_2}} \cdot \frac{\alpha_1}{\alpha_2} \cdot \frac{e_{\beta_1}}{e_{\beta_2}} \qquad \ldots (16)$$

$$\therefore \frac{N_{\gamma_1}}{N_{\gamma_2}} = \frac{A_1'}{A_2'} \cdot \frac{\alpha_1}{\alpha_2} \cdot \frac{e_{\beta_2}}{e_{\beta_1}} \qquad \ldots (17)$$

which is identical to equation (9).

Detectors

The electron detector was a gold-silicon p-n junction type supplied by ORTEC. It has a circular area of 25 mm^2 and the depletion layer at a bias of 200 volts was 400 microns thick, which is the range of a 400 keV electron in silicon. The pulses from this detector were amplified by an ORTEC 103-203 low noise system designed to produce double delay line clipped pulses. This type of pulse was necessary to drive a crossover pickoff fast coincidence unit.

The gamma ray detector was a 1½" diameter by 1" thick NaI(Tl) crystal mounted in an integral line assembly with a Dumont 6292 photo-multiplier tube. Pulses from this unit were fed, via a cathode follower, to a Nuclear Enterprises 5202 double delay line amplifier.

Electronics

Figure 3 shows a block diagram of the electronics used in the sum coincidence experiment. The function of this apparatus was to select those pulses from the electron detector which were in coincidence, i.e. in cascade, with a detected gamma ray, to sum these two pulses and to select only those pulses whose sum fell in a predetermined range. These pulses were then analyzed on a 200 channel analyzer and from the data the ratio of the conversion coefficients of the two

FIGURE 3

Block Diagram of the Electronics

BLOCK DIAGRAM OF THE APPARATUS

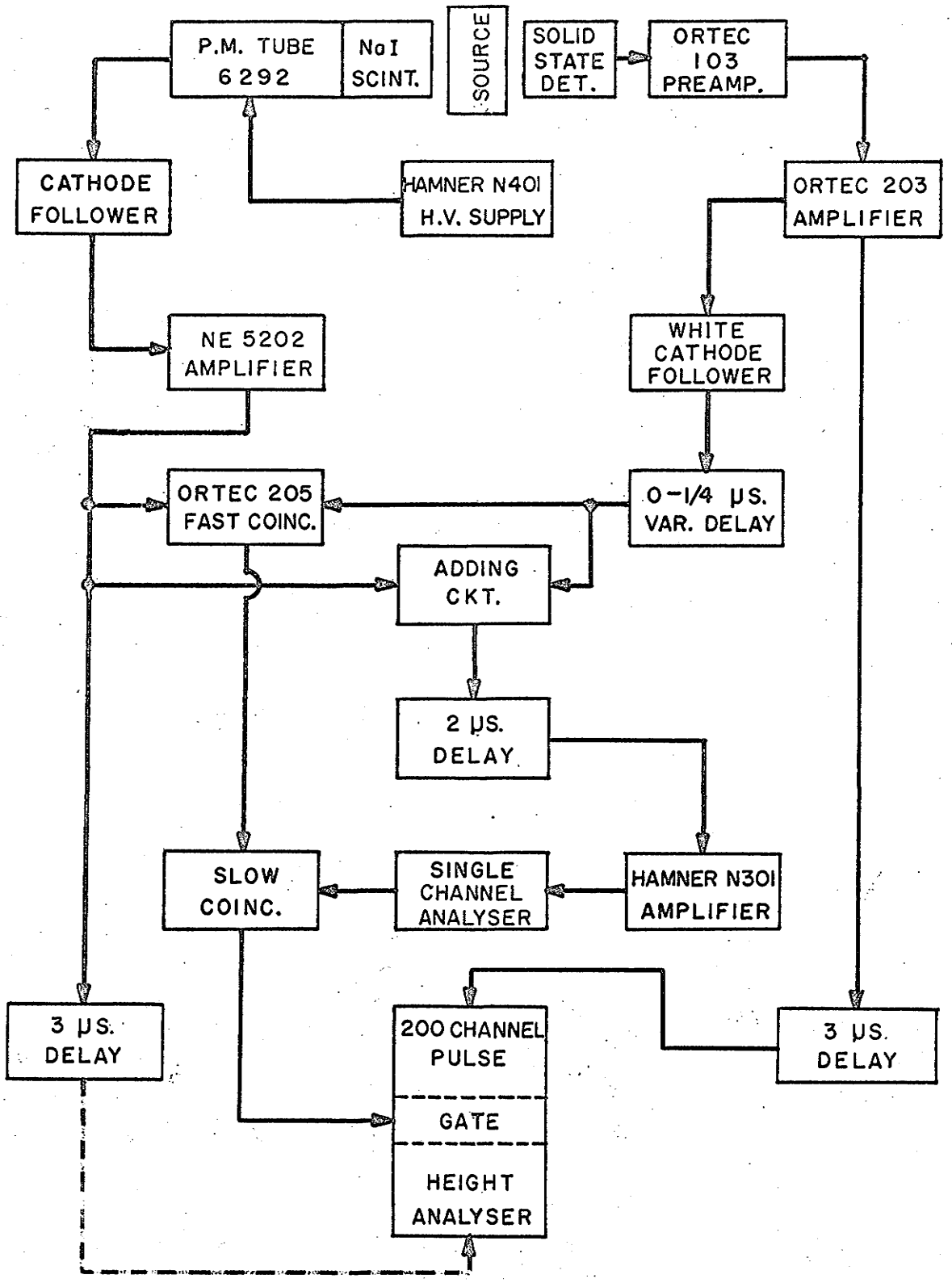

parts of the cascade was calculated using equation (6). Since the ORTEC detection and amplifying system was somewhat faster than the Nuclear Enterprises amplifier, a small delay had to be introduced between the ORTEC amplifier and the ORTEC 205 fast coincidence unit. A typical curve for the setting of this delay is shown in Fig. 4.

In parallel with the fast coincidence unit was a linear adding unit, a circuit diagram of which is given in Fig. 5. The large attenuating resistor was required for pulses from the Nuclear Enterprises amplifier as these signals were much larger than the corresponding pulses from the ORTEC amplifier. The diode was used to eliminate the negative portion of the double delay line signals since this portion created difficulties in the next amplification stage.

The time taken for the ORTEC 205 coincidence unit to give an output pulse from coincident input pulses was 2.0 microseconds, and so the added pulses were delayed by 2.0 microseconds before going to the slow coincidence unit.

The sum pulses were then amplified, to compensate for attenuation in the delay line, and sent to the slow coincidence via a single channel analyzer. This single channel analyzer set the sum level and so the slow coincidence unit triggered only when there was an electron-gamma coincidence which summed

FIGURE 4

Coincidence Counting Rate Versus Delay Line Setting for the 0-0.25 Microsecond Delay Line

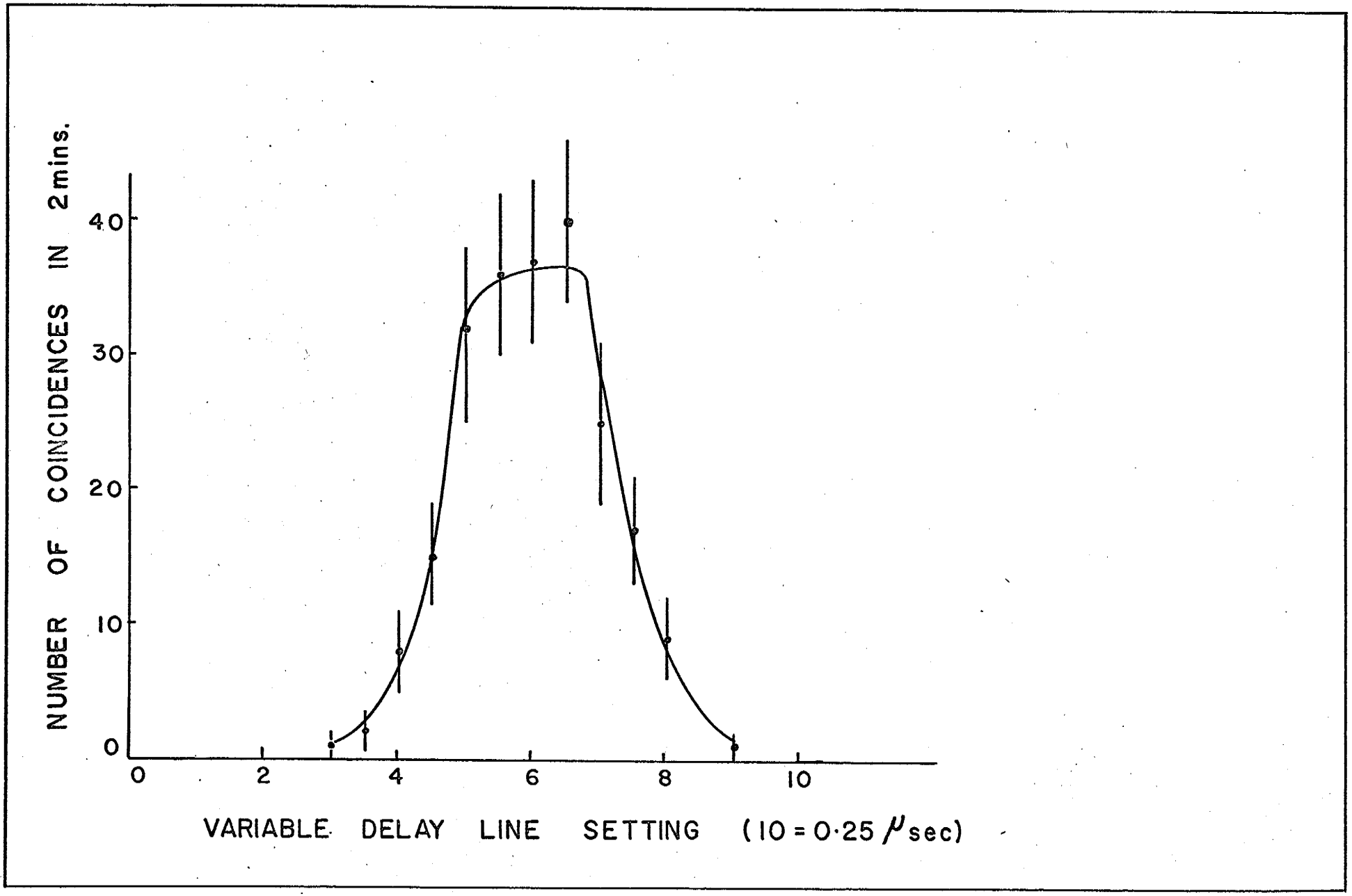
NUMBER OF COINCIDENCES IN 2 mins.
0
10
20
30
40
0
2
4
6
8
10
VARIABLE DELAY LINE SETTING (10 = 0·25 μsec)

FIGURE 5

Circuit Diagram of Adding Unit

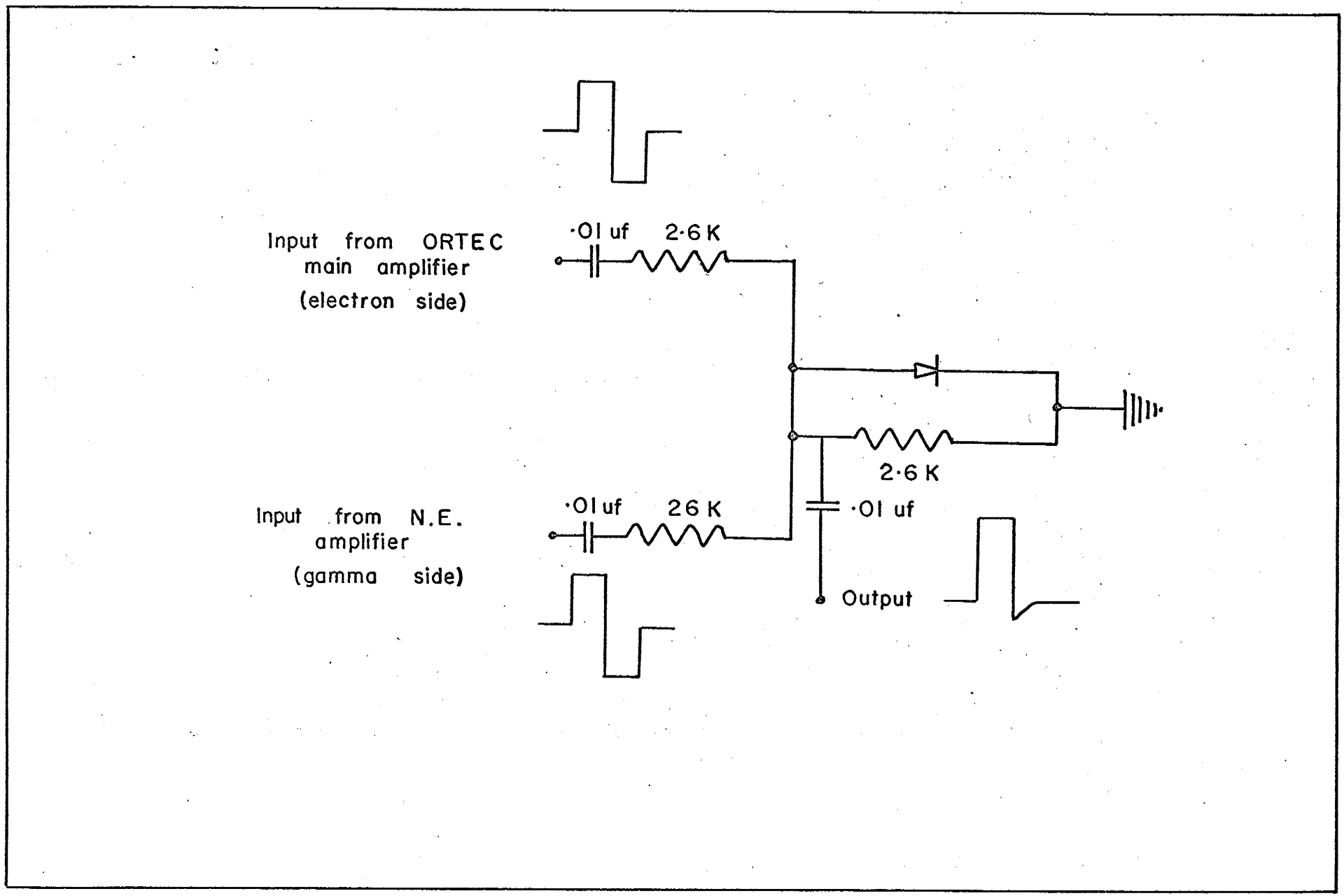
Input from ORTEC main amplifier (electron side)
·01 uf
2·6 K
2·6 K
Input from N.E. amplifier (gamma side)
·01 uf
26 K
·01 uf
Output

to a preset value. The output of this slow coincidence was therefore used as a gate for the 200 channel pulse height analyzer. The latter received its signal pulses from the 203 post amplifier after a 3 microsecond delay to allow for the working time of all the logic circuits.

It was also possible to look at the sum coincidence pulses from the gamma detector, instead of those from the electron detector, and this was done whilst setting up the experiment. However, since the resolution of the pulses from the electron detector was superior to that from the gamma detector, the electron pulses were always analyzed in the sum coincidence experiment.

Setting up of the Electronics

The ORTEC surface barrier detector was used at a bias of 200 volts. The amplification gains on the 103-203 system were changed until both conversion lines of interest could be displayed together on the analyzer. Low bias values were set on the fast coincidence unit and on the single channel analyzer, and with both inputs of the fast coincidence connected to the ORTEC amplifier, the gated electron spectrum was displayed on the 200 channel analyzer. As expected, this spectrum was the same as a singles spectrum indicating that the

delay lines were of the correct length. The lower level of the single channel analyzer was then raised and the readings at which the electron conversion lines were cut off were noted.

This procedure was then repeated for the gamma ray signals from the Nuclear Enterprises amplifier, with the exception that the gain of the amplifier was adjusted so that the gamma rays of the cascade were cut off at the same discriminator settings as were the electron conversion lines.

The apparatus was then reconnected as in Fig. 3 and the single channel analyzer set at a value just above that for a single transition energy, but below that for the sum energy. The 0-0.25 microsecond delay line was then set for the maximum number of gating pulses from the slow coincidence output (see Fig. 4). The single channel analyzer was then set at a value close to the one for the cascade sum and the spectrum viewed on the 200 channel analyzer. A number of spectra were taken at slightly different single channel analyzer settings to ensure that the spectrum did not change with this setting. This ensured that the correct value for the sum level was being used. Fig. 6 shows the variation of sum coincidence areas over a wide range of sum levels.

From these spectra the areas under the conversion peaks were measured and these values were used in equation (6)

17

FIGURE 6

Variation in the Ratio of Sum Coincidence Areas With Sum Level. (The Ratio Shown is for the Areas Under the 136 and 265 keV Peaks for As^{75})

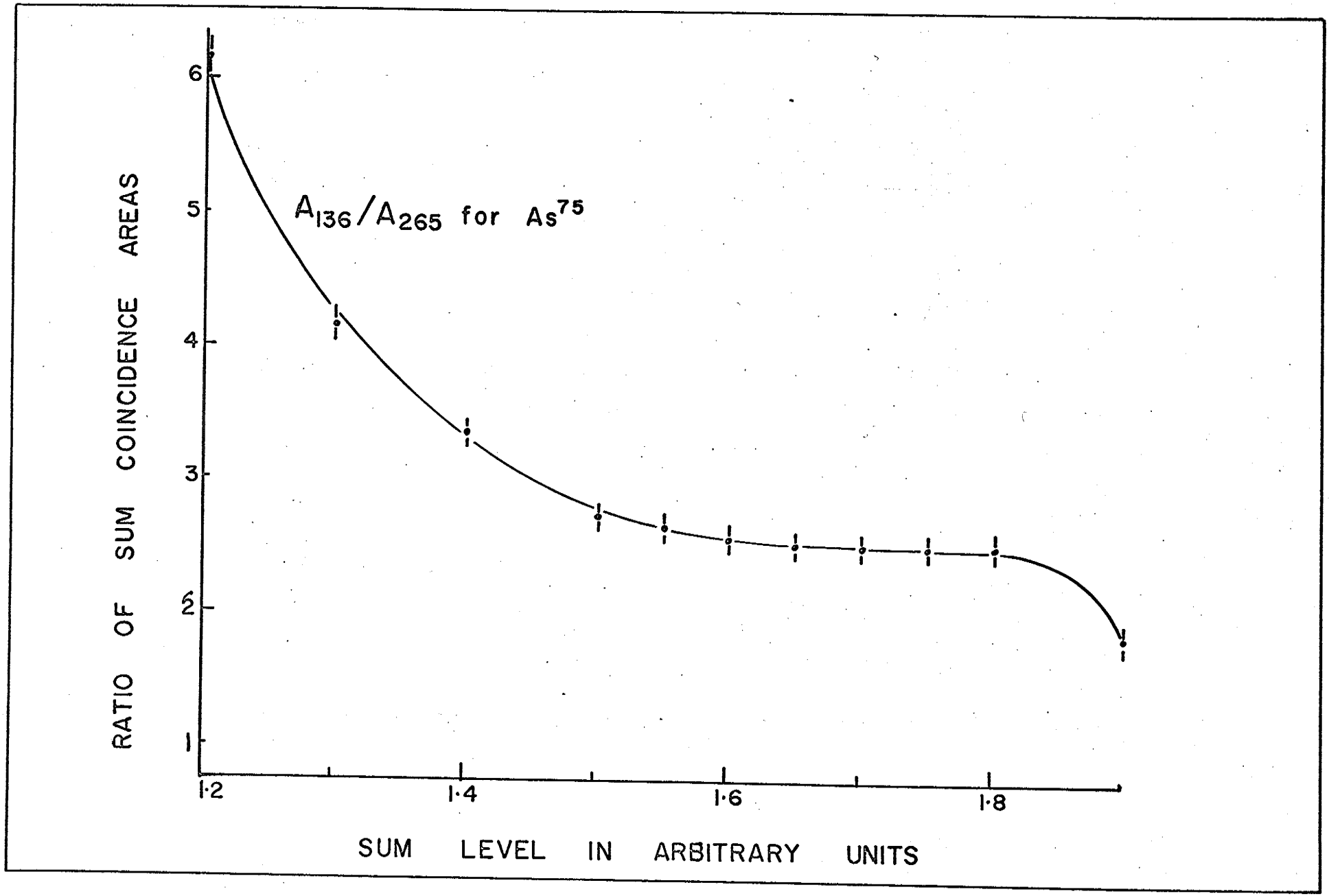
RATIO OF SUM COINCIDENCE AREAS
A_{136}/A_{265} for As^{75}
6
5
4
3
2
1
1·2
1·4
1·6
1·8
SUM LEVEL IN ARBITRARY UNITS

to yield the ratios of the conversion coefficients. However the ratios of the photo-peak and total absorption peak efficiencies of the two detectors at the two energies under investigation had to be known. The efficiencies of the NaI crystal were taken from the Handbuch der Physik[3] and the efficiencies of the electron detector were measured using a beta ray spectrometer (see Part II of this thesis).

Sources

We were limited in our choice of sources by four major considerations.

1) We required a source which decayed by electron capture so that there would be no background beta radiation. This radiation would make background subtraction of the singles spectra very difficult and would also partially invalidate equation (6).

2) Conversion electrons should have energies within the energy range from 60 to 500 keV. The lower limit was set by the rapid build up of pulses due to backscattering of the electrons from the detector and thus distorting the conversion peak; the upper limit was set by the depletion depth of the detector (see Part II).

3) The transition energies of the cascade should differ by about 50 keV so that the conversion lines from each

transition could be separately resolved.

4) It was necessary to have as large an intensity as possible for the cascade transitions in order that counting times should not be longer than 2 days to get approximately 10,000 counts in one of the conversion peaks.

Two sources were chosen which satisfied these requirements and they were Se^{75} (120 days) and Ba^{131} (12 days) which decay, by electron capture, to excited states of As^{75} and Cs^{131} respectively. The levels of As^{75} had been thoroughly investigated recently[4,5] and hence provided us with a guide as to whether this method was feasible, whereas information on the excited levels of Cs^{131} was sparse and quite old[6,7] and we hoped to provide useful information on this isotope.

The isotopes were obtained from Oak Ridge National Laboratory U.S.A. as chlorides dissolved in concentrated hydrochloric acid. Their specific activities were 7.6 mc/ml for the Se^{75} and 0.15 mc/ml for the Ba^{131}.

Source Preparation

One drop of the radioactive source solution was dried at the centre of a gold plated V.Y.N.S. film which was supported on an aluminum planchette ring. Details of the preparation of the source backing and gold plating are given in a previous thesis from this department[8].

Experimental Chamber

A plan view of the chamber is shown in Fig. 7. The aluminum planchette source rings were held vertically in the vacuum chamber about 1 cm. from the solid state electron detector. The NaI gamma detector was just outside the chamber and viewed the source through the hemispherical aluminum cap. The chamber was evacuated using a Balzers rotary pump and a liquid nitrogen trap was used to condense any oil vapour which may otherwise have found its way into the chamber. This precaution was taken because the surface of the gold silicon detector is said to be sensitive to oil vapour which may cause a breakdown in its electrical properties.

FIGURE 7

Experimental Chamber

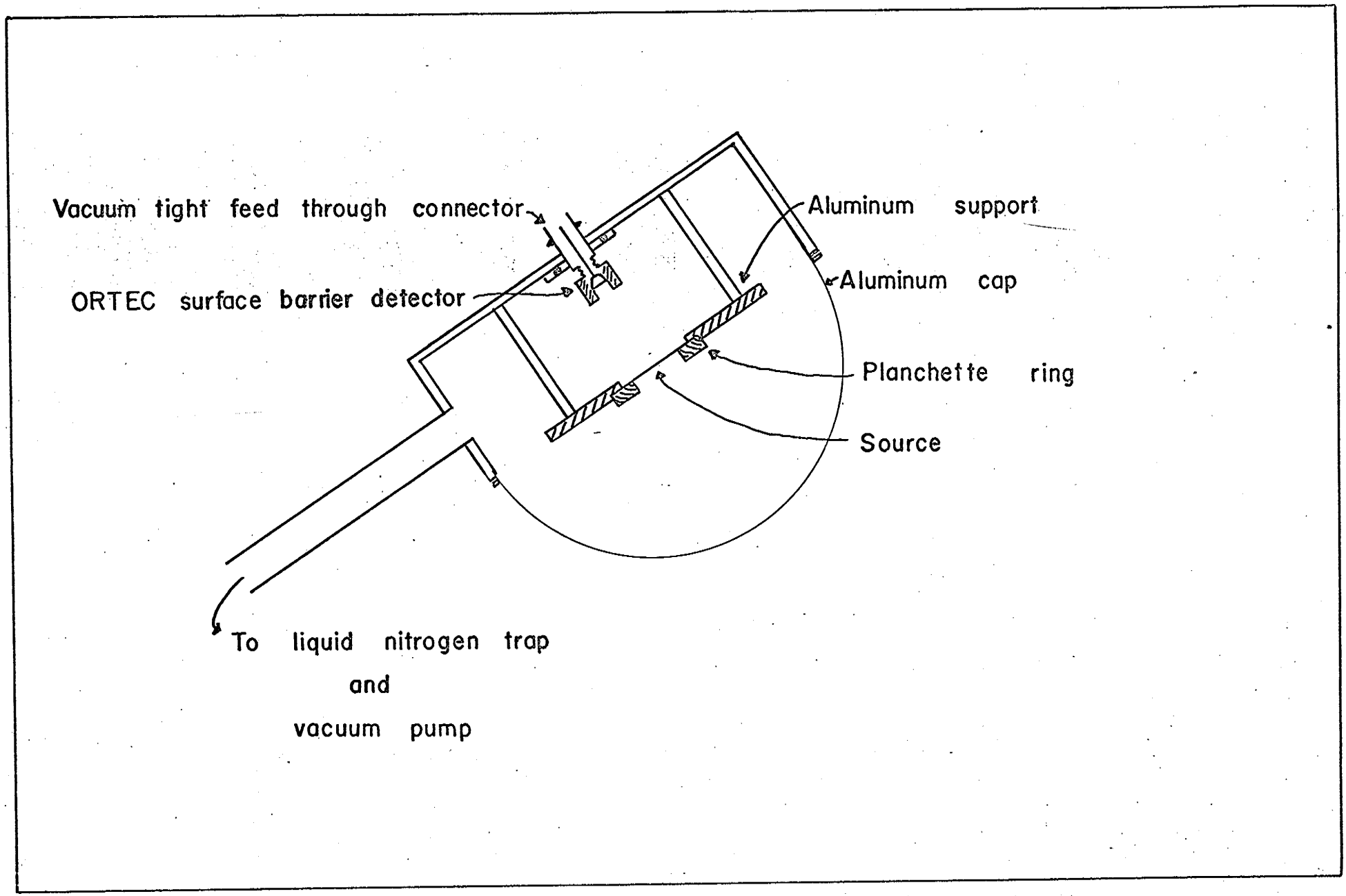
Vacuum tight feed through connector
ORTEC surface barrier detector
Aluminum support
Aluminum cap
Planchette ring
Source
To liquid nitrogen trap
and
vacuum pump

RESULTS ON As^{75}

The presently accepted level scheme for As^{75} is shown in Fig. 8. The cascades investigated were those between the 401 keV level and the ground state.

The sum coincidence experiment was run for periods of 20 hours and at the end of each run a singles spectrum of pulses from the electron detector was taken for 2 hours. Singles and sum coincidence curves for conversion electrons from transitions in the excited states of As^{75} are shown in Figs. 9 and 10. There are three cascades between the 401 keV level and the ground state but the 96 keV - 305 keV cascade does not appear in the sum coincidence spectrum as the 305 keV level has a lifetime of 3 milliseconds. The other two cascades between the 401 keV level and the ground state are separated by only 15 keV, which is approximately equal to the resolution of the detector. Hence the two pairs of peaks are not fully resolved. This required us to strip off the two smaller areas from the larger ones before we could measure their areas. We did this by insisting that the curves should be symmetrical and have equal F.W.H.M. as measured in keV.

The results of this work on the levels of As^{75} are given in Tables 1, 2 and 3. Table 1 gives the ratios of the total internal conversion coefficients of the two cascades which

FIGURE 8

Decay Scheme of $Se^{75} \longrightarrow As^{75}$. Energies given in keV.

(Taken from Nuclear Data Sheets)

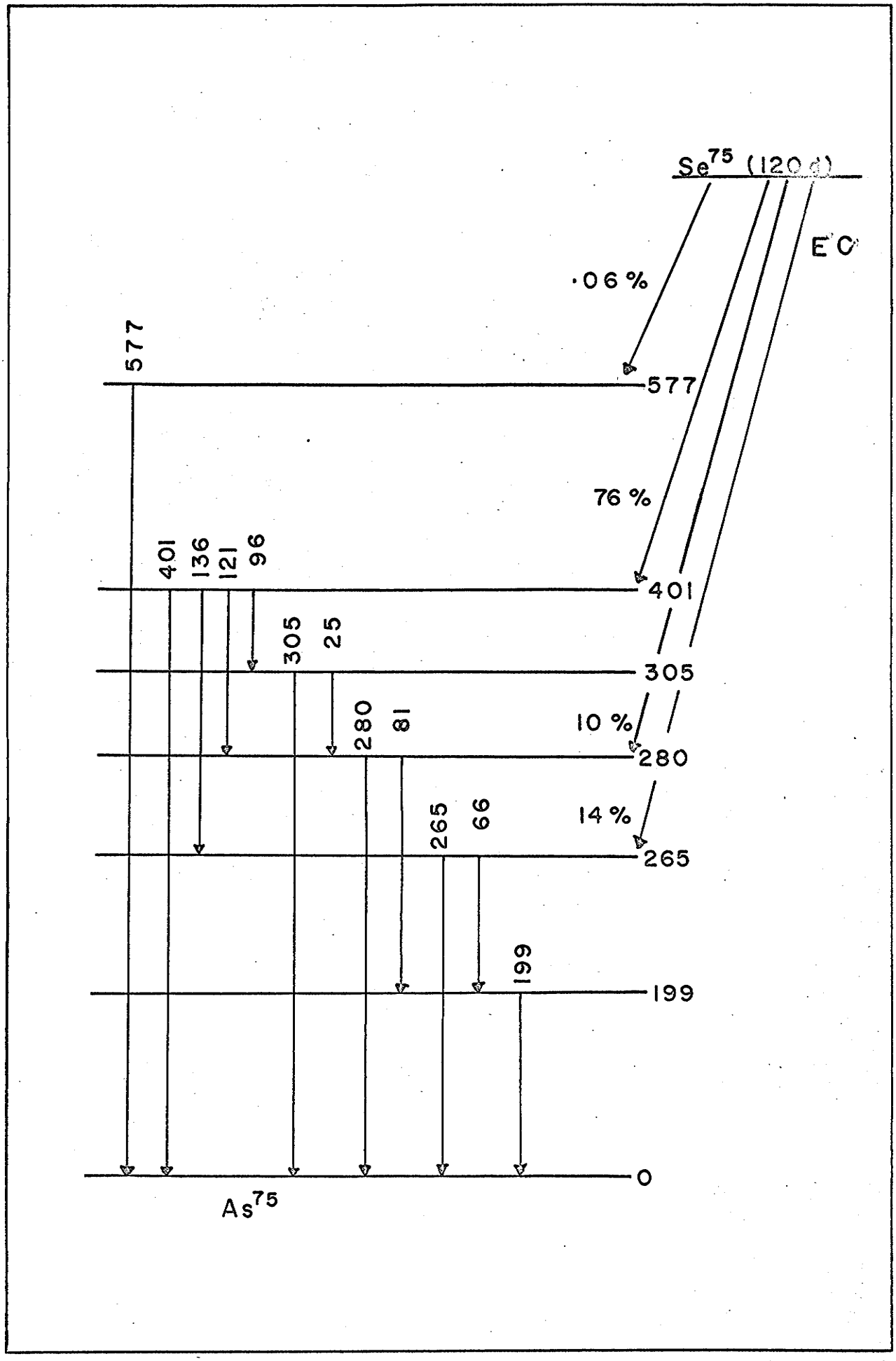
Se^{75} (120 d)
E C
·06 %
76 %
10 %
14 %
577
401
305
280
265
199
0
577
401
136
121
96
305
25
280
81
265
66
199
As^{75}

FIGURE 9

Conversion Electron Singles Spectrum for As^{75}

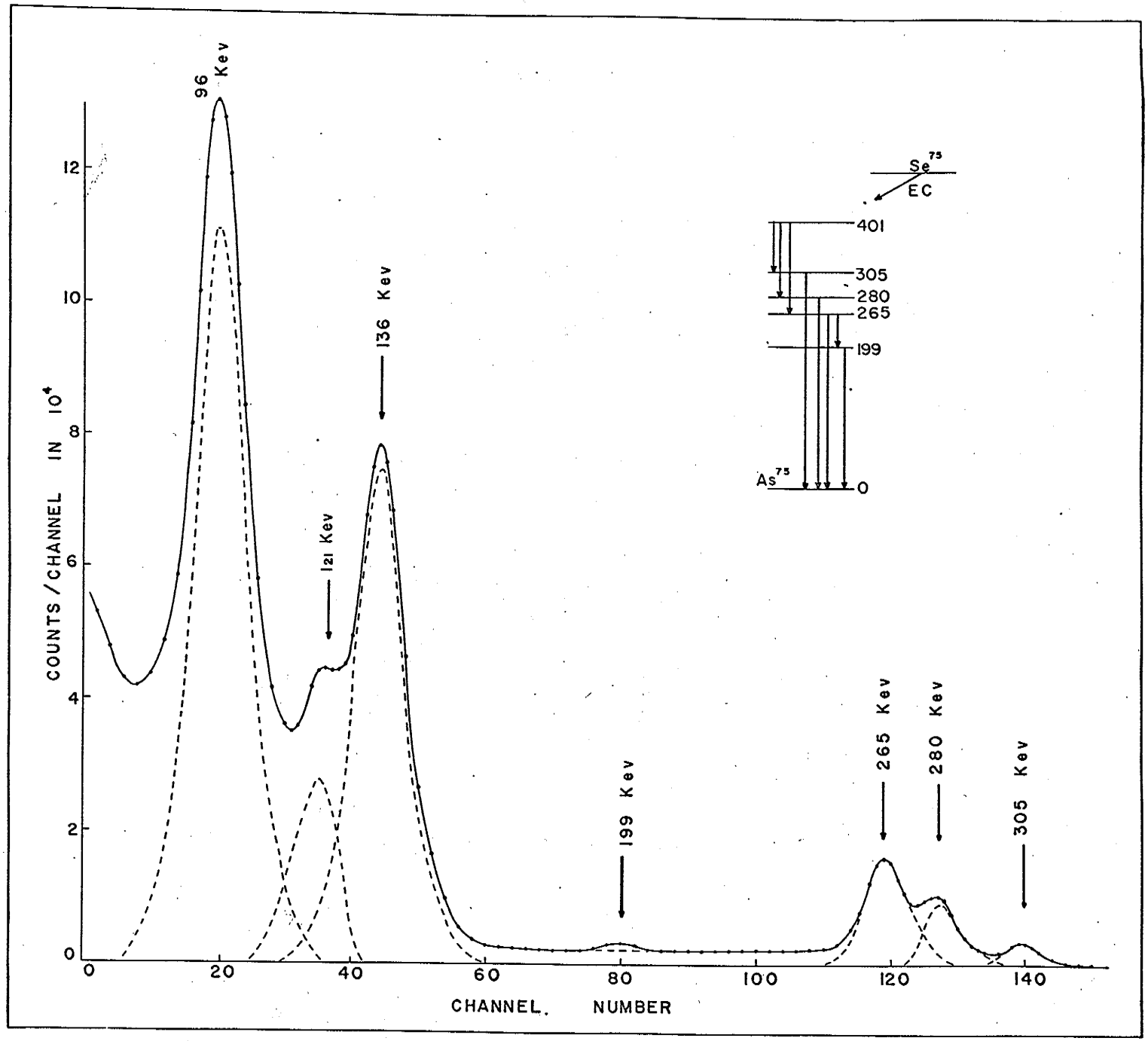

Conversion electron spect

FIGURE 10

Sum Coincidence Electron Spectrum for As^{75}

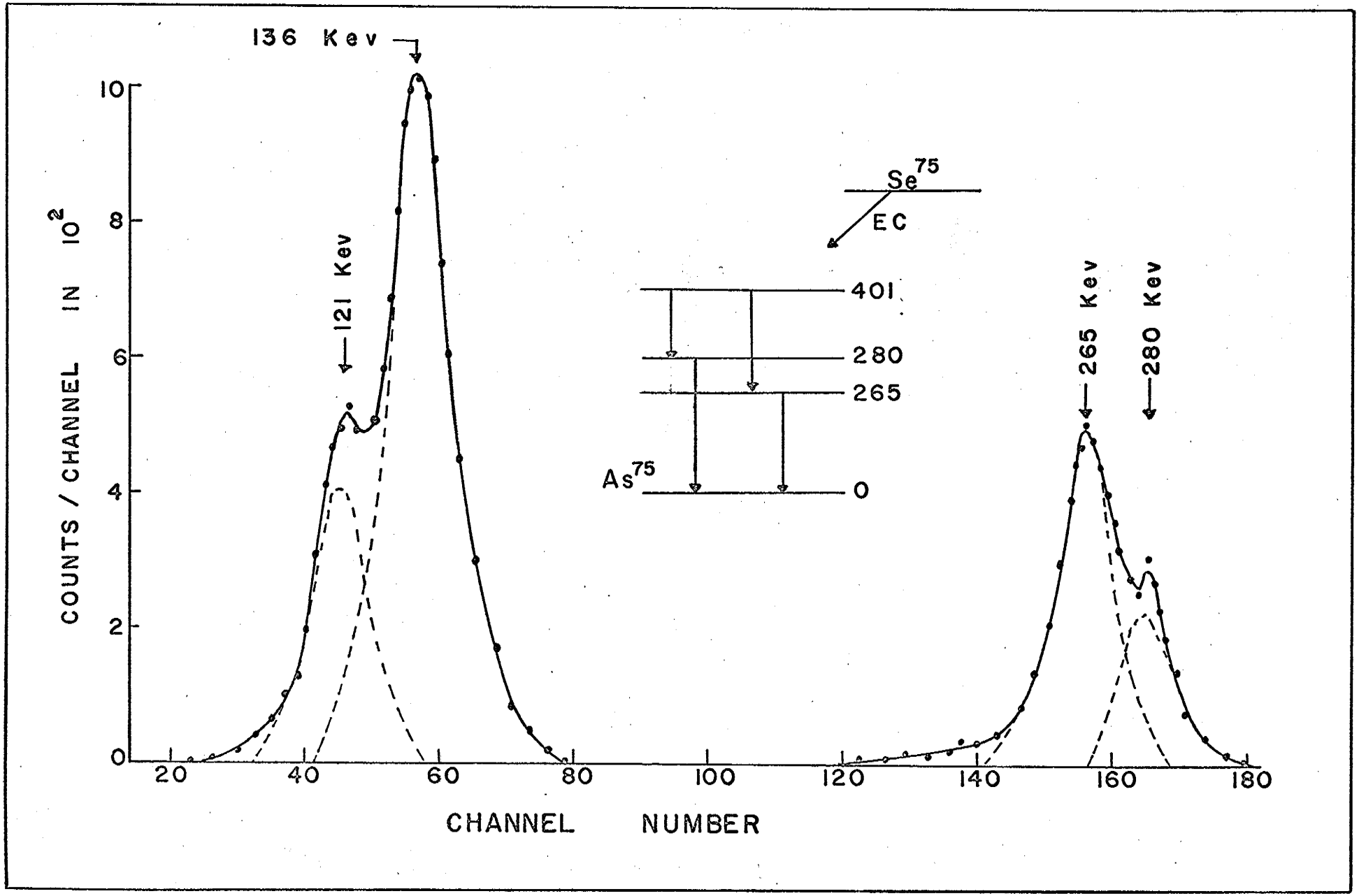

Sum coincidence spectrum

TABLE 1

RATIOS OF TOTAL INTERNAL CONVERSION COEFFICIENTS

Quantity	Edwards and Gallagher	Grigorev and Zolotavin	Present Work
$\frac{\alpha_{121}}{\alpha_{280}}$	5.2 ± 0.6	4.7 ± 0.7	5.5 ± 0.6
$\frac{\alpha_{136}}{\alpha_{265}}$	4.1 ± 0.3	4.2 ± 0.5	4.0 ± 0.3

TABLE 2

RELATIVE INTERNAL CONVERSION ELECTRON INTENSITIES

Transition energy (keV)	Edwards and Gallagher	Grigorev and Zolotavin	Present Work
96	795 ± 60	660 ± 45	750 ± 75
121	187 ± 15	154 ± 7	167 ± 20
136	391 ± 30	378 ± 15	520 ± 50
199	7 ± 1	7.1 ± 0.3	7 ± 1
265	100	100	100 ± 10
280	55 ± 5	49 ± 4.0	52 ± 5
305	17.4 ± 1.7	16.2 ± 1.0	17 ± 2

TABLE 3

RELATIVE GAMMA RAY INTENSITIES

Transition energy (keV)	Edwards and Gallagher	Grigorev and Zolotavin	Present Work
121	28.0 ± 0.6	27.9 ± 1.3	30 ± 10
136	95.5 ± 1.8	96 ± 5	130 ± 40
265	100	100	100
280	42.2 ± 0.6	41 ± 2.5	53 ± 15

were investigated. Our values of 5.5 ± 0.6 and 4.0 ± 0.3 agree well within the experimental errors involved, with the other investigators [4,5]. The experiments of Edwards and Gallagher and those of Grigorev and Zolotavin were done using beta ray spectrometers. The relative internal conversion electron intensities for the 7 transitions which we identified are given in Table 2. These also show agreement with the other investigators except for the intensity of the 136 keV conversion line which appears to be too high.

The relative gamma ray intensities, calculated from Tables 1 and 2 using equation (7) in the theory section, are shown in Table 3. These show agreement, within our rather large errors, with the previously reported results, which have been found by direct measurement.

The errors on the values of the ratios of the conversion coefficients accumulate from three sources:-

i) measurement of the relative areas on Fig. 10;

ii) measurement of the relative efficiencies of the electron detector; and

iii) values of the relative efficiencies of the NaI crystal. The error due to i) was reduced to 4% or less by repeated experiments. The error in ii) and iii) was estimated to be approximately 2% for each ratio. This gave us a total

error of about 8% for the 136 keV - 265 keV cascade (the more intense of the two) and about 10% for the 121 keV - 280 keV cascade. The 10% errors in relative electron intensities in Table 2 arise from difficulties of background subtraction and the more difficult unfolding of the curves in Fig. 9. The errors, in Table 3, of the gamma ray intensities are the composite sum of the other errors.

RESULTS ON Cs^{131}

The presently accepted level scheme for Cs^{131} is shown in Fig. 11. The cascades investigated were those between the 620 keV level and the ground state. Of the four such cascades the only one which we identified was the 496 keV - 124 keV cascade. The other cascades from this level are down in intensity by a factor of 20 times or more[9] compared to this cascade.

Sum coincidence spectra were taken for periods of 20 hours and at the end of each run a singles spectrum of pulses from the electron detector was taken for 2 hours. Singles and sum coincidence spectra for conversion electrons from transitions in the excited states of Cs^{131} are shown in Figs. 12 and 13. Figure 12 also contains two lines, K-276 and L+M-276, of Ba^{133m} which was contained as an impurity in the original solution. It was found to disappear quite rapidly in comparison to the Cs^{131} lines since Ba^{133m} has a half life of 39 hours, compared to 12 days for Ba^{131}.

It can also be seen from Figs. 12 and 13 that the 496 keV conversion lines appear narrower than the other peaks. This is due to the fact that the ORTEC amplifier was working near the maximum pulse height limit and was non-linear in this region. It was however ascertained that the area under these

FIGURE 11

Decay Scheme of $Ba^{131} \longrightarrow Cs^{131}$. Energies Given in keV.

(Taken From Nuclear Data Sheets)

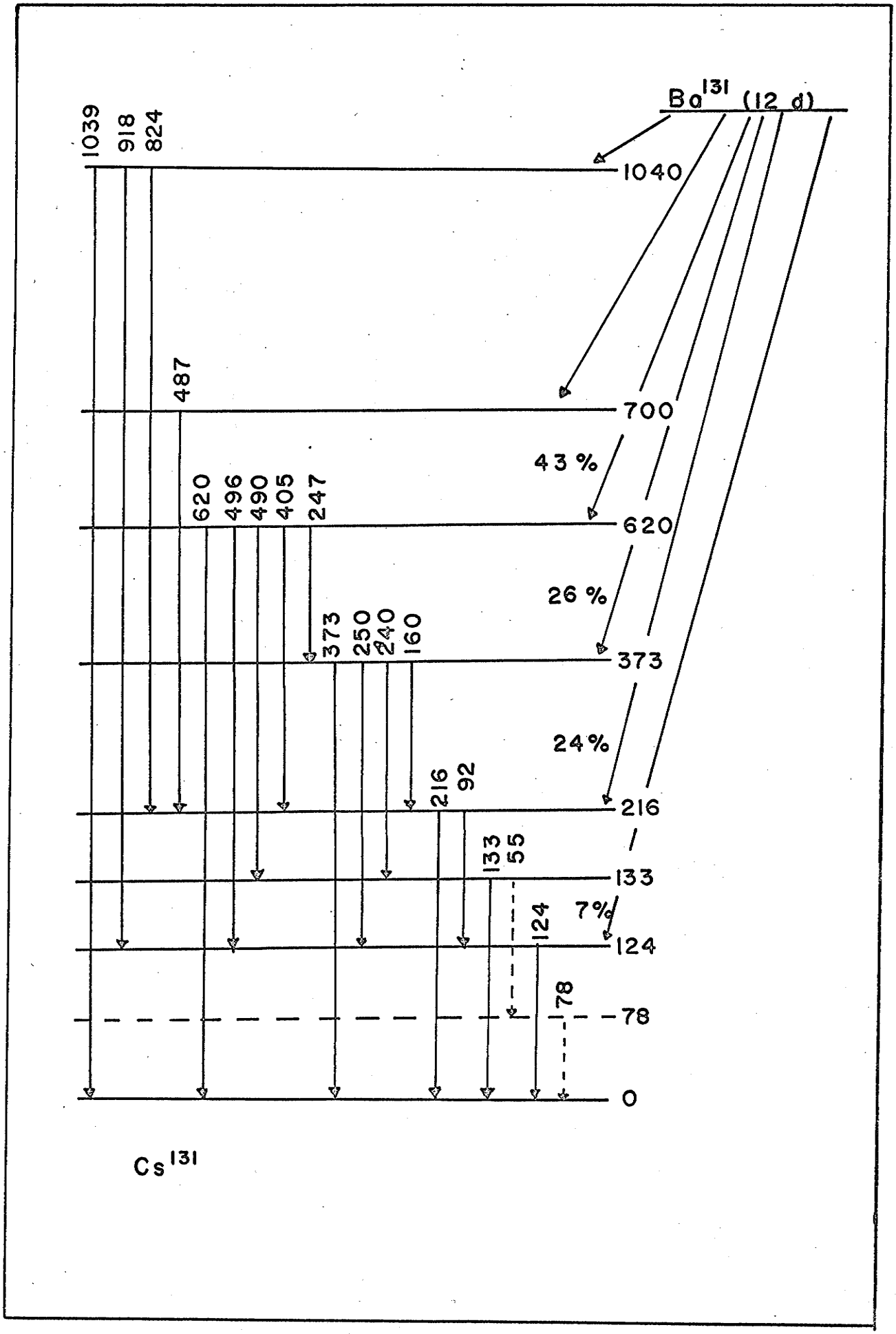
Ba 131 (12 d)
1039
918
824
1040
487
700
43 %
620
496
490
405
247
620
26 %
373
250
240
160
373
24 %
216
92
216
133
55
133
7%
124
124
78
78
0
Cs 131

FIGURE 12

Conversion Electron Singles Spectrum for Cs^{131}

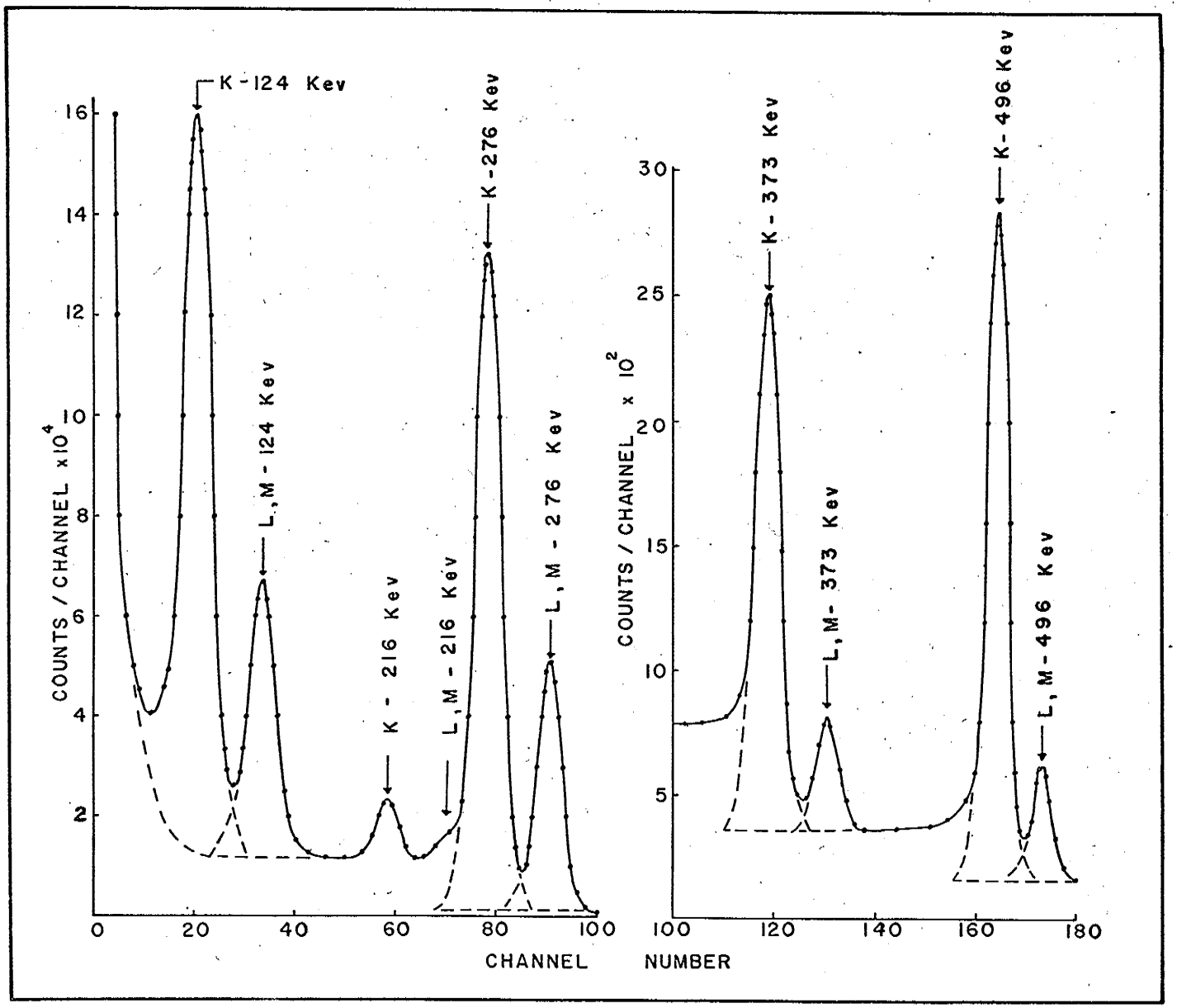

Conversion electron spectrum of Cs^{131}

FIGURE 13

Sum Coincidence Electron Spectrum for Cs^{131}

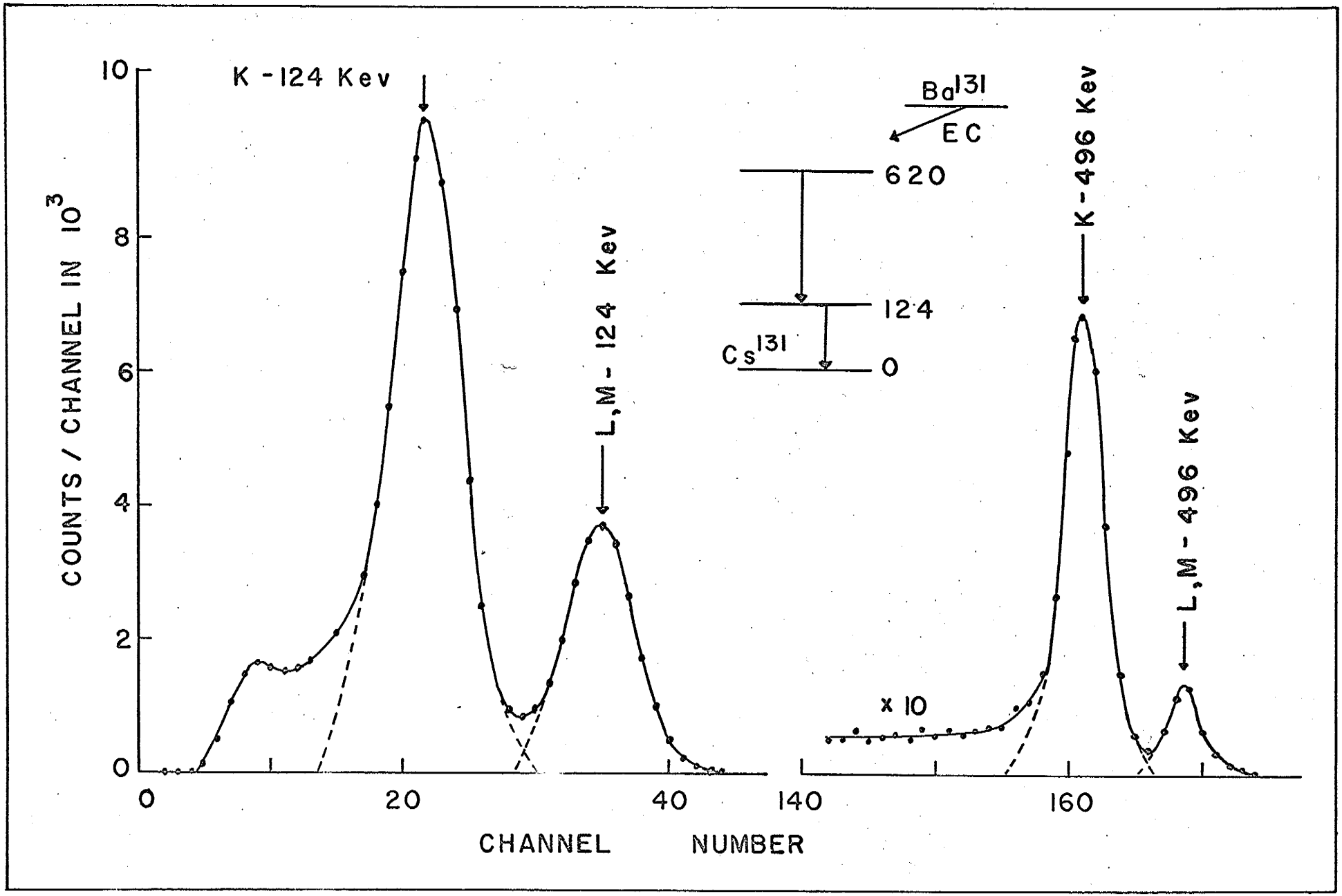

Sum coincidence spectrum

peaks remained constant when the amplification was reduced and these peaks taken out of this non-linear portion of the spectrum.

The results of the work on the excited levels of Cs^{131} are given in Tables 4, 5, 6 and 7. We obtain a value of 65 ± 5 for the ratio of the K conversion coefficients of the 124 and 496 keV transitions. There is no previous reference to this except that of a recently published paper by Kelly and Horen[9]. (This paper came to our attention after we had completed our work). From the paper by Kelly and Horen[9] we have calculated two values for this ratio, one directly from the ratio of conversion electron intensities to the ratio of gamma ray intensities, which came out to be 65 (no errors are quoted on these measurements), the other from the ratio of their calculated conversion coefficients which was 60 ± 25. This work of Kelly and Horen was done using a beta ray spectrometer.

The K to L + M conversion ratios given in Table 5 were measured for both singles and sum coincidence spectra. These values are compared with other published values[6, 7, 9]. It can be seen that our values are self consistent and agree with those of Kelly and Horen[9] except for the 216 keV transition. It is found for this transition that there is a contribution

TABLE 4

RATIO OF K CONVERSION COEFFICIENTS

Quantity	Kelly and Horen		Present Work
	Direct Calculation	From their calculated values for the coefficients	
$\frac{\alpha_{124}}{\alpha_{496}}$	65	60 ± 25	65 ± 5

TABLE 5

K/ (L+M) CONVERSION RATIOS

Transition energy (keV)	Elliott et al*	Cork et al*	Kelly and Horen	Present Work	
				Sum Coincidence	Singles
124	6.0 ± 0.5	3.6 ± 0.3	2.4	2.5 ± 0.2	2.7 ± 0.3
216	2.8 ± 0.4	9 ± 2	6.5	-	3.1 ± 0.3
373	-	6 ± 0.5	4.1	-	4.6 ± 0.5
496	2.5 ± 0.8	7.7 ± 0.5	6.0	6.0 ± 0.5	6.2 ± 0.6
276**	-	-	-	-	2.7 ± 0.3

* These values are quoted as K/L in the original papers.

** From Ba^{133m} (39 hr.) impurity.

TABLE 6

RELATIVE K CONVERSION ELECTRON INTENSITIES

Transition energy (keV)	Kelly and Horen	Present Work
124	100	100
216	10.2	8.7 ± 0.5
373	1.6	1.5 ± 0.1
496	2.7	1.8 ± 0.1

TABLE 7

RELATIVE GAMMA RAY INTENSITIES

Transition energy (keV)	Kelly and Horen	Present Work
124	100	100
496	170	120 ± 20

to the 216 L+M conversion peak due to K conversion from the 239 keV transition and if allowance is made for this using the results of Kelly and Horen then the two sets of data for the K/L+M ratios are in agreement.

Table 6 shows the relative K conversion electron intensities compared to the only other published data and these values agree except for the value of the conversion electron intensity of the 496 keV transition which we have found to be some 30% lower than that of Kelly and Horen. Our value for the relative gamma ray intensity as calculated from Tables 4 and 6 is given in Table 7. This also shows a discrepancy of some 30% in the relative intensities of the 496 keV transition.

Discussion of Part I

The work presented here has shown that the sum coincidence technique for the determination of the ratios of conversion coefficients is a very successful method. In the particular cases of measurements on the two isotopes described, it is probably one of the best presently available methods. We did, however, limit ourselves to electron capture sources and to transition energies between 100 and 500 keV and had we stepped outside these limitations to beta active sources, then the experiment would be less accurate because of the difficulty in background subtraction. However, they would theoretically still be capable of producing good results. The limitations on transition energy were set by the type of electron detector available.

The recent technological advances in the production of solid state detectors have made it possible to extend the upper energy limit to 2 MeV, though with some loss in energy resolution.

P A R T II

ABSTRACT

Some work has been done using mono-energetic beams of electrons selected by a Siegbahn-Slätis beta ray spectrometer to study the variation of the absorption efficiency of a gold silicon surface barrier detector with energy and depletion depth. It is shown that there is a continuous decrease of peak efficiency with increasing electron energy, and that the total efficiency remains constant, close to 100%, for a wide range of energies and depletion depths. Work was also carried out to determine the sensitivity of the electron detector to gamma radiation.

INTRODUCTION

According to equation (6) on Page 6 in Part I, a knowledge of the peak efficiency of the gold silicon electron detector is required[10] for the determination of the ratios of the conversion coefficients. This part of the Thesis contains the measurements of the efficiency of the electron detector together with other information concerning the detector.

The peak efficiency of the detector as a function of energy was measured in two parts. Firstly the total efficiency, which was found to be 100% in the energy range in which we were interested, and secondly the peak-to-total ratio.

MEASUREMENT OF TOTAL EFFICIENCY

A Siegbahn-Slätis beta ray spectrometer was used to focus mono-energetic beams of electrons onto the detector. The detector was mounted on the pole plug of the spectrometer in such a way that it could be moved on all three axes so that the position of the active area of the detector could be adjusted until it lay at the focal point of the spectrometer.

The beta spectra of several radioactive sources were then found using both the solid state detector and either a geiger counter, for energies less than 100 keV, or a scintillation counter for energies greater than 100 keV. Both the latter counters are assumed to be 100% efficient for their particular energy ranges and so we compared the counting rates of the detectors at the peaks of the conversion lines of the sources. There was found to be no consistent discrepancy at any energy and we assumed the total efficiency of the Au-Si detector to be 100% up to 800 keV. Further, measurement of the variation of total efficiency with depletion depth was made by focussing a mono-energetic beam of electrons onto the detector and finding the change in the total number of counts. (In a surface barrier detector of this type the depletion depth is proportional to the square root of the bias voltage).

This change in total number of counts is shown in Fig. 14 together with the peak to total ratios measured in the same experiment. Both curves are for an incident electron energy of 320 keV.

Figure 14 shows that electrons of this energy produce measurable pulses in the detector down to a bias of about 30 volts. This bias is equivalent to the range of a 190 keV electron and we think, therefore, that the total efficiency of the detector at 200 volts bias will remain constant up to incident electron energies of 700 keV, i.e. 1.7 times the energy of electrons which are totally absorbed in the detector.

FIGURE 14

Total and Peak to Total Efficiencies as a Function of Bias Voltage. Incident Electron Energy 320 keV.

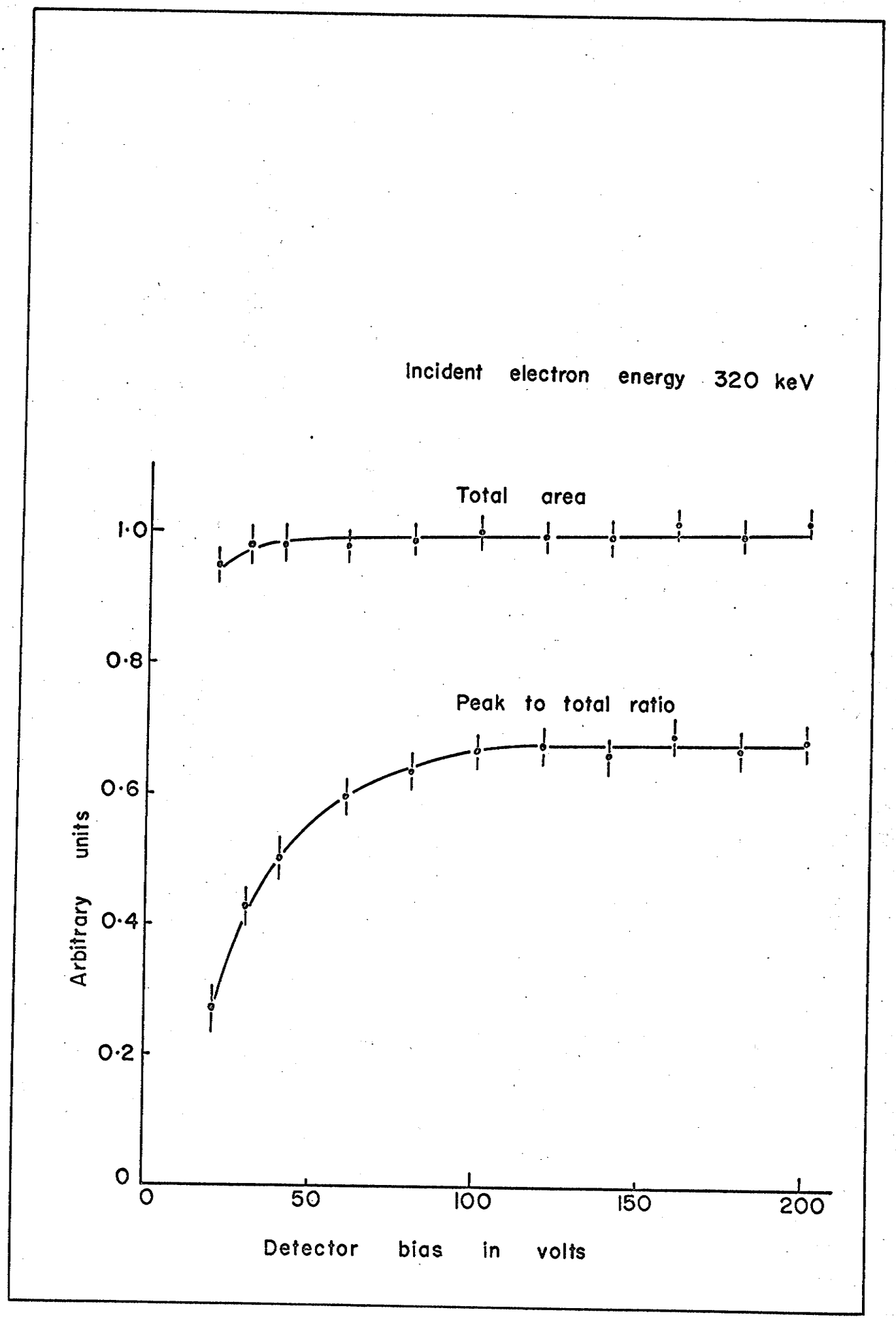
Incident electron energy 320 keV
Total area
Peak to total ratio
1·0
0·8
0·6
0·4
0·2
0
Arbitrary units
0
50
100
150
200
Detector bias in volts

MEASUREMENT OF PEAK TO TOTAL RATIOS

The second part of the efficiency measurement, peak to total ratios, was carried out also using the beta ray spectrometer. The sources of electrons for this experiment were Ce^{141} and Cs^{134} deposited on gold plated V.Y.N.S. films as mentioned in Part I of this Thesis. The mono-energetic beams of electrons selected by the beta ray spectrometer and focussed onto the surface of the detector yielded a pulse height distribution which was displayed on a 400 channel analyzer. Typical pulse height spectra, normalized to constant total area, for some incident electron energies are shown in Fig. 15. The detector bias for these spectra was 200 volts, the same as that used in the sum coincidence experiments described in Part I, giving rise to a depletion depth of 410 microns. This depletion depth corresponds to the range of a 400 keV electron in silicon. Under the best operating conditions full width half maximum (F.W.H.M.) for the detector and amplifying system was about 15 keV.

Two important characteristics may be observed in Fig. 15:

i) the height of the peaks gradually decreased with energy even when the detector depletion depth was thick enough

FIGURE 15

Normalized Pulse Height Spectra for Different Incident Energies Taken at a Bias of 200 Volts

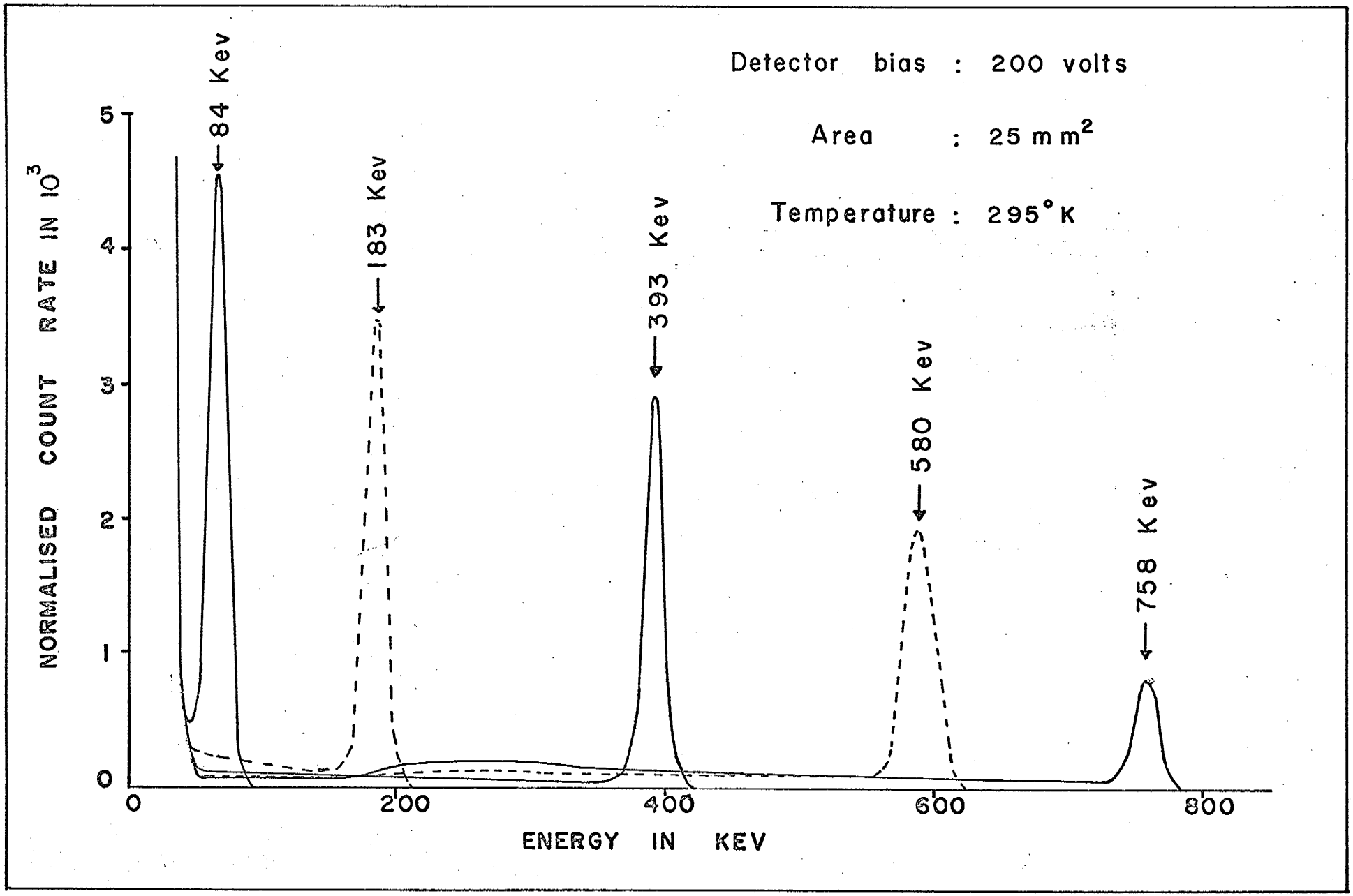

Electron energy spectrum

to stop the most energetic electrons.

ii) the width of the total absorption peak for electrons whose range exceeds the depletion layer of the detector is much broadened.

The first point is due to the fact that at higher incident energies the more is the number of electrons scattered out of the detector and hence the reduction in the number of electrons in the total absorption peak. Figure 16 shows the ratio of the area under the total absorption peak to the total area as determined from the curves in Fig. 15. The peak to total ratio is seen to vary only slightly for electrons in the energy range 150 to 400 keV and to fall off sharply for electrons of energy greater than 400 keV. As mentioned previously, electrons of energy 400 keV have a range in silicon equal to the depletion depth of the detector at a bias of 200 volts. The widening of the total absorption peak at energies above 400 keV is due to the escape of a number of the scattered electrons out of the detector. The values of F.W.H.M. and peak to total ratios at various incident energies are given in Table 8.

FIGURE 16

Peak to Total Ratio as a Function of Incident Energy

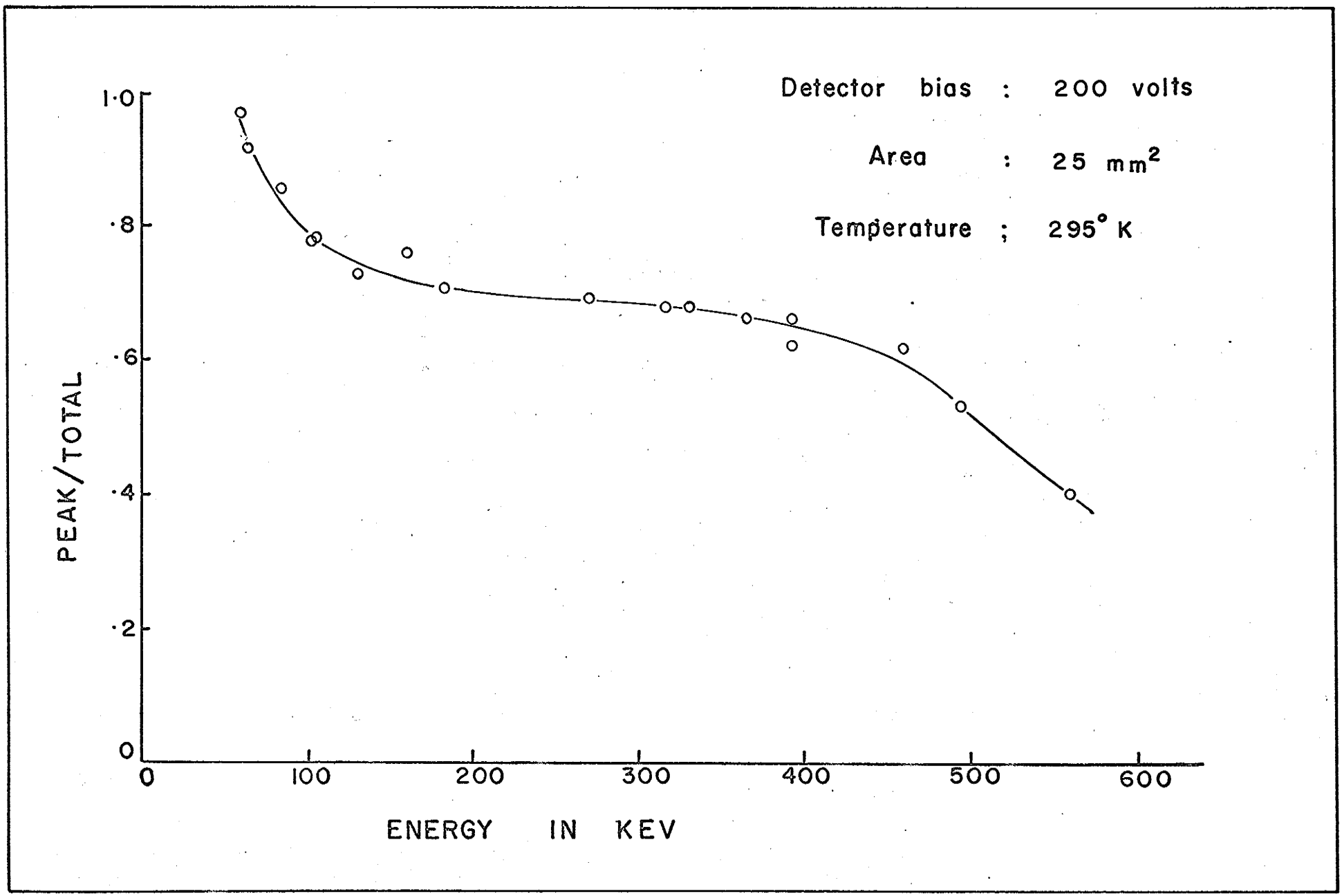

Beta efficiency curve

TABLE 8

RESPONSE OF THE GOLD SILICON DETECTOR AT DIFFERENT BIAS VOLTAGES AND INCIDENT ENERGIES

Detector Bias								
200 Volts			50 Volts			20 Volts		
Energy (keV)	Peak Total	FWHM (keV)	Energy (keV)	Peak Total	FWHM (keV)	Energy (keV)	Peak Total	FWHM (keV)
62	0.86	17	166	0.77	20	72	0.92	20
183	0.71	18	265	0.68	22	122	0.75	23
393	0.63	19	313	0.53	30	247	0.54	25
494	0.53	27	445	0.21	28	374	0.16	27
580	0.40	27	568	0.11	27	391	0.10	30
758	0.19	25	---	----	--	---	----	--

SOME MEASUREMENTS AT THIN DEPLETION DEPTHS

We also investigated the pulse height spectrum produced in the detector by mono-energetic electrons when most of them were passing through the detector. Since we had no intense source of high energy electrons, energies greater than 800 keV, we reduced the depletion depth of the detector so that it corresponded to the range of a 200 keV electron. We did this by reducing the bias voltage to 50 volts. A set of pulse height spectra produced in the detector by mono-energetic beams of electrons, normalized to constant area, is shown in Fig. 17. At energies above 300 keV most electrons passed through the detector and deposited only a small fraction of their energy. Consequently, a broad secondary peak appeared at a lower energy. The position of this peak moved to the left as the energy of the incident beam increased indicating that the energy for minimum ionization, about 600 keV, had not yet been reached.

It was also noticed that the F.W.H.M. for the peaks corresponding to incident electrons whose range exceeds the depletion layer of the detector is much broadened. Figures for this are given in Table 8 together with similar information for detector biases of 200 volts and 20 volts.

FIGURE 17

Normalized Pulse Height Spectra for Different Incident Energies Taken at a Bias of 50 Volts

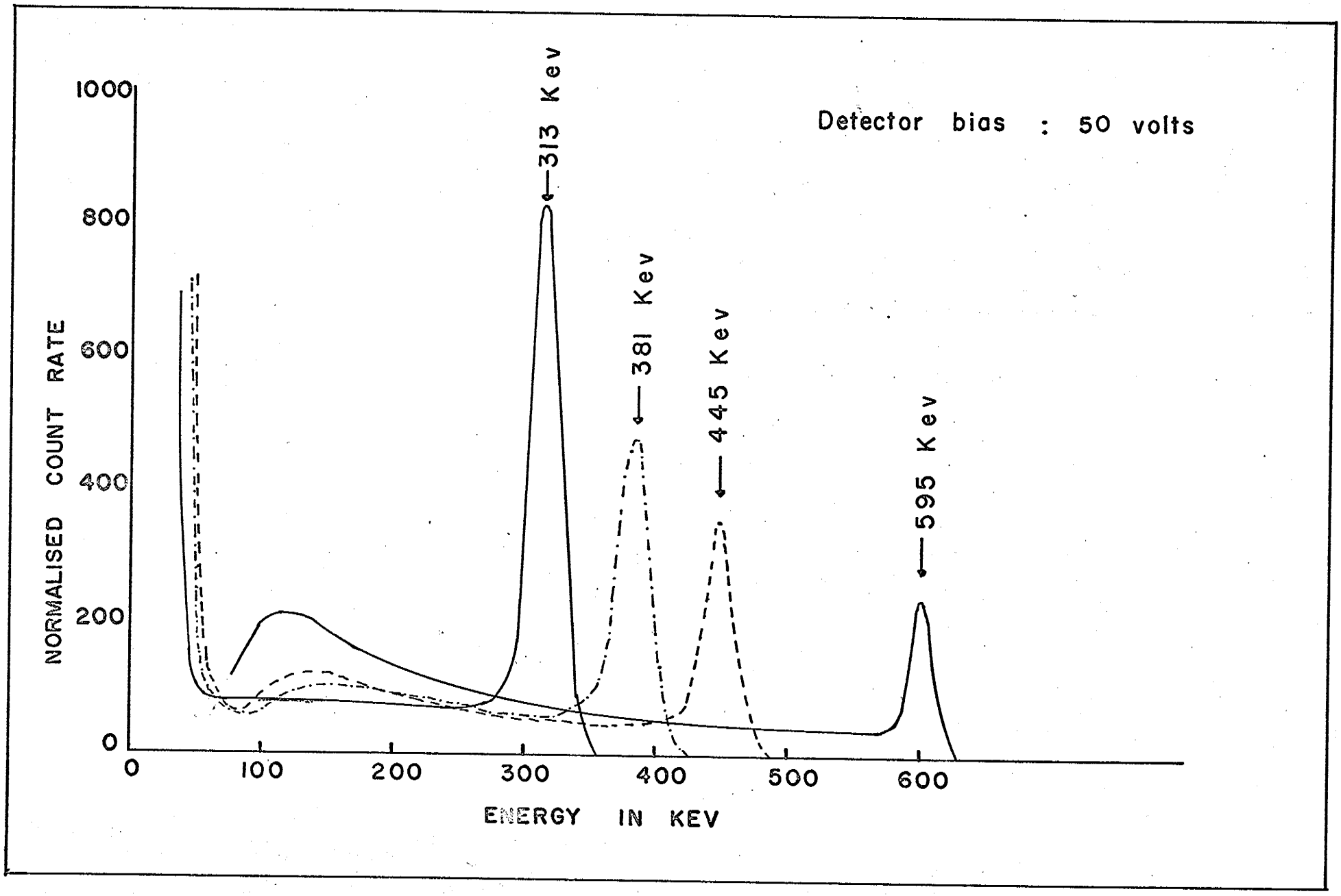

Electron energy spectrum

It was also noticed as shown in Fig. 17 that the number of small pulses (corresponding to a detected energy of 30 to 70 keV) increased quite rapidly as the number of electrons traversing the detector increased. This is shown more clearly in Fig. 18 where the energy scale has been considerably expanded. The upper curves show the low energy part of the spectrum for energies which are totally absorbed in the detector. The low energy 'elbow' of these curves appears to be at approximately the same energy for all three incident energies. This is not true for the curves shown in the lower part of Fig. 18. In this set of curves the incident energy of the electrons was sufficiently high so that most of the electrons passed through the detector. The cause of this shift is not fully understood although we think it is probably due to the combined effect of backscattering from the surface and the shifting and rising of the low energy broad secondary peak with increasing energy. It is not due to noise and is unlikely to be pulses from electrons which have passed through the detector because the probability of these electrons leaving a pulse smaller than those in the broad transmission peak is very slight.

FIGURE 18

Low Energy Pulse Height Spectra at a Bias of 50 Volts

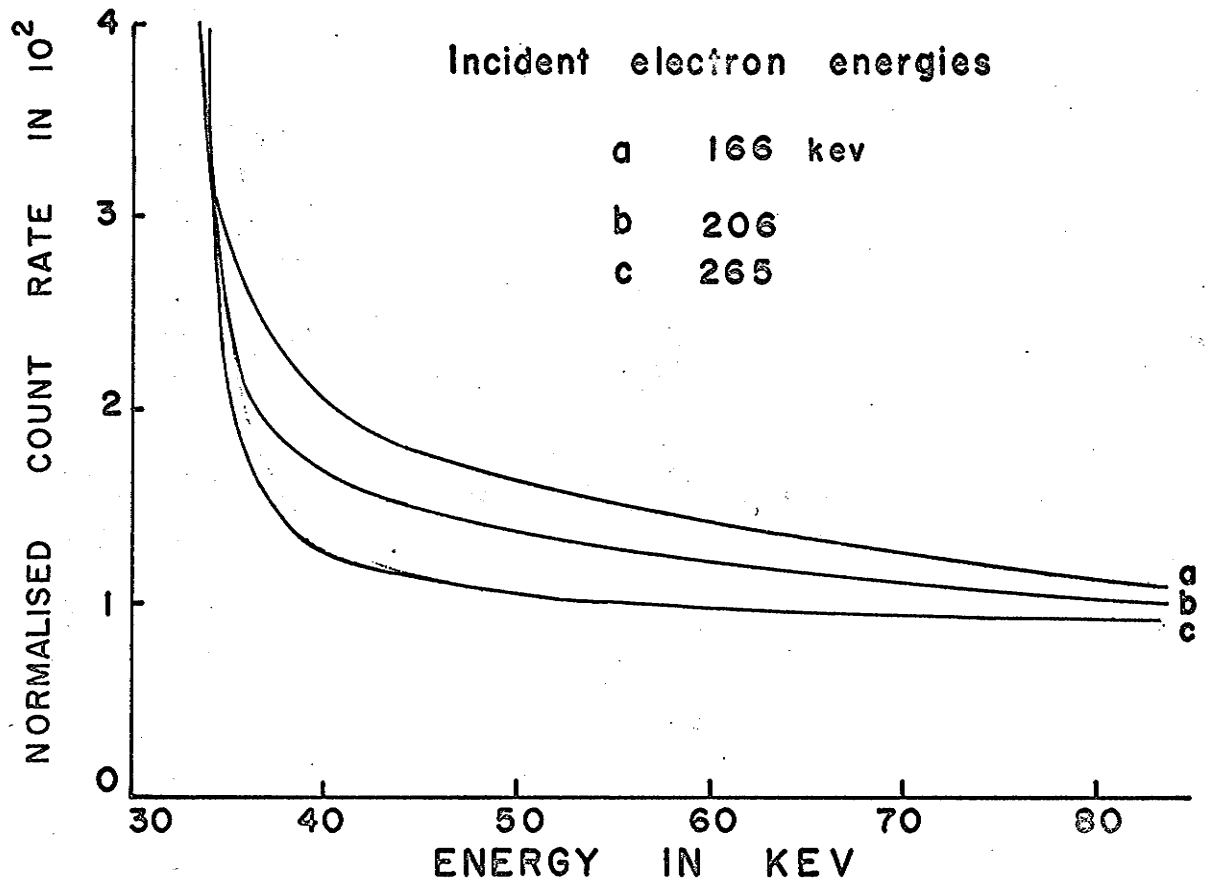

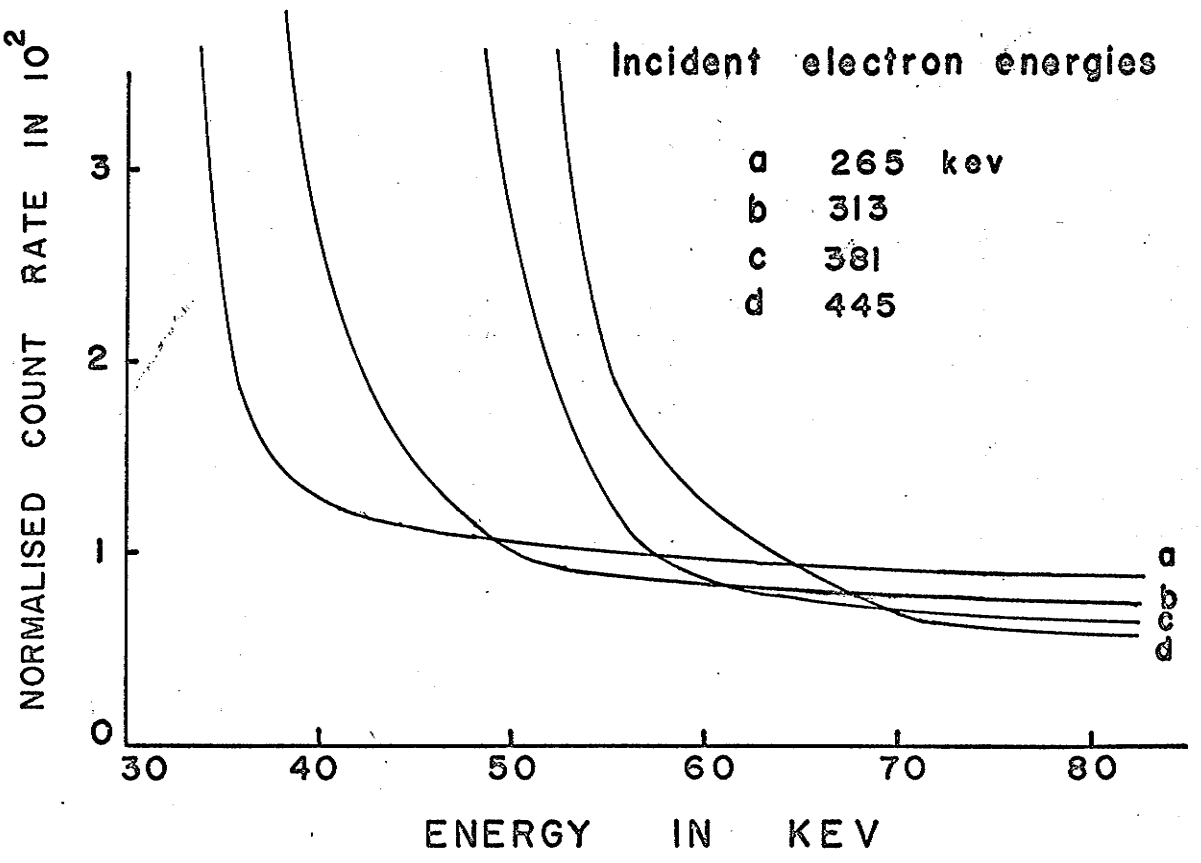

Low energy electron spectrum 50 volts bias

GAMMA RAY SENSITIVITY

One of the properties of this detector, as can be seen from Fig. 15, is the essentially uniform background produced by beams of mono-energetic electrons. This means, that for elements decaying by electron capture, background subtraction for a conversion electron spectrum is a relatively simple and accurate manipulation. This would not be the case if the number of pulses from the detector due to Compton interactions with gamma rays became a significant part of the spectrum. This is shown in Fig. 19 showing the pulse height spectrum produced by Cr^{51}. This spectrum was taken in the experimental chamber not in the beta ray spectrometer. The large area on the left is due to Compton interactions with the 323 keV gamma ray whilst the peak on the right is from the conversion electrons of this transition. The gamma interactions are visible here only because the conversion coefficient of this transition is very small, .0015, and the number of gamma rays striking the detector is 700 times the number of electrons. From this the smallest conversion coefficient which can be measured without having to make a correction for this effect has been estimated to be .005.

Compton scattering of gamma rays has also been observed when positrons were fired into the detector by the beta

FIGURE 19

Pulse Height Spectrum Produced by the Decay of $Cr^{51} \rightarrow V^{51}$

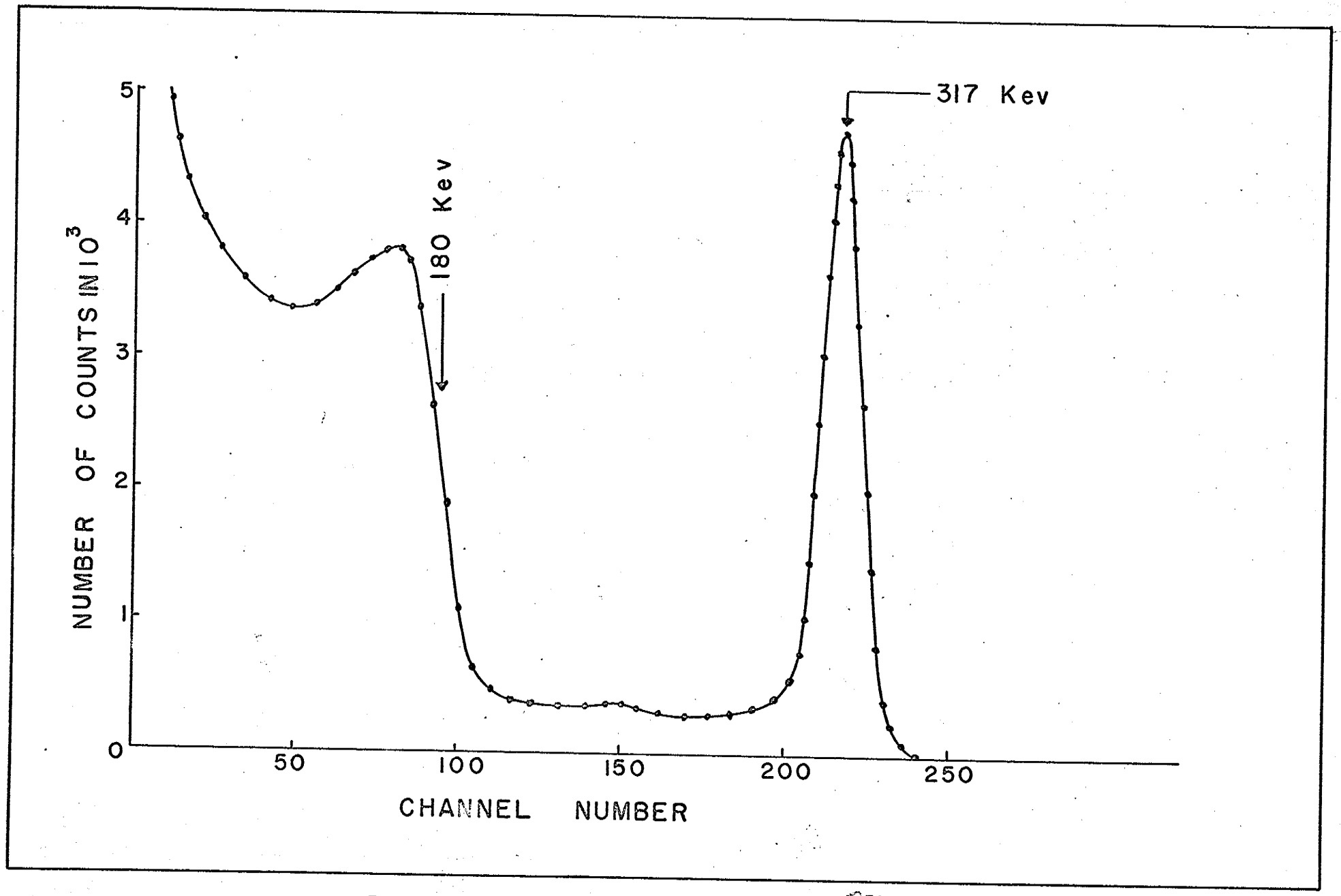

Pulse height spectrum of Cr^{51}

ray spectrometer. In this case there is a high energy tail on the positron spectrum due to Compton scattering of the .511 MeV annihilation gamma ray. This is shown in Fig. 20. This figure shows the pulse height spectrum produced for two different incident positron energies. The energy difference between the peak and the edge of the tail is approximately constant at 325 keV, the maximum energy of a Compton electron scattered by a .511 MeV annihilation gamma ray.

FIGURE 20

Pulse Height Spectra Produced by Positrons

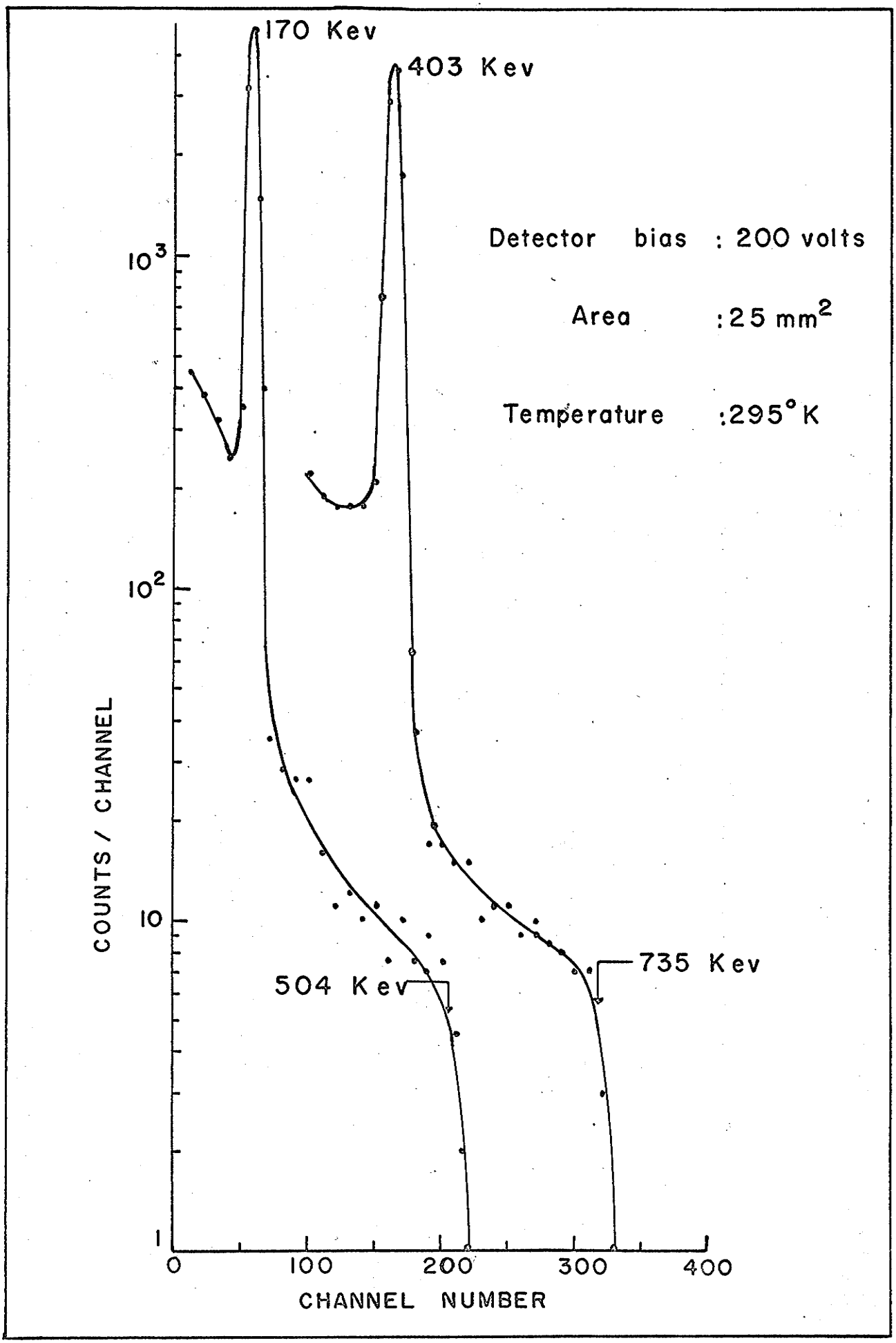

Positron spectrum

Discussion of Part II

The situation with regard to the use of silicon surface barrier diodes for electron, or positron, detection, as shown in this work, is that except for very low energy electrons, the peak efficiency of the detector is never greater than 70% mainly because of backscattering out of the detector. It also shows that there is a continuous decrease of total absorption peak efficiency with energy. This is not in agreement with the work of McKenzie and Ewan[11], who found that this remained constant up to 350 keV. (At this energy the electrons had a range equal to the depletion depth of their detector).

Although the detector response is linear[10], the peak efficiency for electrons which are able to penetrate the detector depletion depth decreases sharply and the F.W.H.M. of the peaks is broadened by about 30%. Also the low energy tail of the spectrum is distorted by backscattering and this sets a lower limit on the energies of electron conversion lines, in this case about 60 keV, below which there would be considerable distortion of these peaks.

REFERENCES

1. S. K. Sen: Seminar, Physics Dept., University of Manitoba November 1961.

2. S. K. Sen and B. G. Hogg: Nuclear Instruments and Methods 15 (1962) 209.

3. W. E. Mott and R. B. Sutton: Nuclear Instrumentation II, Handbuch der Physik Volume XLV (1958).

4. W. F. Edwards and C. J. Gallagher: Nuclear Physics 26 (1961) 649.

5. E. P. Grigorev and A. V. Zolotavin: Nuclear Physics 14 (1959) 443.

6. J. M. Cork, J. M. LeBlanc, W. H. Nester and M. K. Brice: Phys. Rev. 91 (1953) 76.

7. M. W. Elliott, L. S. Cheng, J. R. Haskins and J. D. Kurbatov: Phys. Rev. 88 (1952) 263.

8. W. J. Keeler: M.Sc. Thesis University of Manitoba (1964).

9. W. H. Kelly and D. J. Horen: Nuclear Physics 47 (1963) 454.

10. S. K. Sen: Nuclear Instruments and Methods 27 (1964) 74.

11. J. M. McKenzie and G. T. Ewan: I.R.E. Transactions on Nuclear Science NS-8 (1961) 50.